

การเตรียมเส้นใยไทเทเนียมไดออกไซด์สำหรับใช้เป็นวัสดุภาคนึ่งในโครมาโทกราฟีแบบแผ่นบาง

นางสาวสุภมาส กาญจนกุลกุล

วิทยานิพนธ์นี้เป็นส่วนหนึ่งของการศึกษาตามหลักสูตรปริญญาวิทยาศาสตรมหาบัณฑิต

สาขาวิชาปิโตรเคมีและวิทยาศาสตร์พอลิเมอร์

คณะวิทยาศาสตร์ จุฬาลงกรณ์มหาวิทยาลัย

ปีการศึกษา 2554

ลิขสิทธิ์ของเอกสารฉบับนี้สงวนไว้สำหรับวิทยานิพนธ์  
บทคัดย่อและแฟ้มข้อมูลฉบับเต็มของวิทยานิพนธ์ตั้งแต่ปีการศึกษา 2554 ที่ให้บริการในคลังปัญญาจุฬาฯ (CUIR)

เป็นแฟ้มข้อมูลของนิสิตเจ้าของวิทยานิพนธ์ที่ส่งผ่านทางบัณฑิตวิทยาลัย

The abstract and full text of theses from the academic year 2011 in Chulalongkorn University Intellectual Repository (CUIR) are the thesis authors' files submitted through the Graduate School.

PREPARATION OF TITANIUM DIOXIDE FIBERS AS STATIONARY PHASE IN  
THIN LAYER CHROMATOGRAPHY

Miss Supamas Kanjanakunthon

A Thesis Submitted in Partial Fulfillment of the Requirements  
for the Degree of Master of Science Program in Petrochemistry and Polymer Science

Faculty of Science

Chulalongkorn University

Academic Year 2011

Copyright of Chulalongkorn University

Thesis Title	PREPARATION OF TITANIUM DIOXIDE FIBERS AS STATIONARY PHASE IN THIN LAYER CHROMATOGRAPHY
By	Miss Supamas Kanjanakunthon
Field of Study	Petrochemistry and Polymer Science
Thesis Advisor	Puttaruksa Varanusupakul, Ph.D.
Thesis Co-advisor	Nipaka Sukpirom, Ph.D.

---

Accepted by the Faculty of Science, Chulalongkorn University in Partial  
Fulfillment of the Requirements for the Master's Degree

..... Dean of the Faculty of Science  
(Professor Supot Hannongbua, Dr.rer.nat.)

#### THESIS COMMITTEE

..... Chairman  
(Assistant Professor Warinthorn Chavasiri, Ph.D.)

..... Thesis Advisor  
(Puttaruksa Varanusupakul, Ph.D.)

..... Thesis Co-advisor  
(Nipaka Sukpirom, Ph.D.)

..... Examiner  
(Assistant Professor Varawut Tangpasuthadol, Ph.D.)

..... External Examiner  
(Assistant Professor Jinda Yenyongchaiwat, Ph.D.)

สุภมาส กาญจนกุลณฑล: การเตรียมเส้นใยไทเทเนียมไดออกไซด์สำหรับใช้เป็นวัฏภาคนิ่งในโครมาโทกราฟีแบบแผ่นบาง. (PREPARATION OF TITANIUM DIOXIDE FIBERS AS STATIONARY PHASE IN THIN LAYER CHROMATOGRAPHY) อ. ที่ปรึกษาวิทยานิพนธ์หลัก: ดร.พุทธรักษา วรานุศุภากุล, อ. ที่ปรึกษาวิทยานิพนธ์ร่วม: ดร.นิปกา สุขภิรมย์, 68 หน้า.

ในงานวิจัยนี้ได้เตรียมเส้นใยไทเทเนียมไดออกไซด์ด้วยเทคนิคอิเล็กโทรสปินนิงผ่านกระบวนการโซลเจล โดยทำการศึกษาปัจจัยที่เกี่ยวข้องกับลักษณะโครงสร้างพื้นฐานของเส้นใยที่เกิดขึ้นจากกระบวนการอิเล็กโทรสปินนิง พบว่าศักย์ไฟฟ้า ระยะห่างจากเข็มถึงฉากรองรับและอัตราการไหลของสารละลายมีผลต่อขนาดของเส้นใย นอกจากนี้เมื่ออัตราส่วนของพอลิไวนิลไพร์โรลิโดนต่อไทเทเนียมไดออกไซด์สูงขึ้น ได้ขนาดของเส้นใย พื้นที่ผิว และขนาดรูพรุนลดลง เมื่ออุณหภูมิที่ใช้ในการเผาเส้นใยสูงขึ้น ได้ขนาดของเส้นใยและพื้นที่ผิวลดลง ขนาดรูพรุนใหญ่ขึ้น และเริ่มเกิดการเปลี่ยนโครงสร้างของไทเทเนียมไดออกไซด์จากอะนาเทสเป็นรูไทล์ เส้นใยที่เตรียมได้มีขนาดเส้นผ่านศูนย์กลาง 50-190 นาโนเมตร และมีพื้นที่ผิวจำเพาะ 2-34 ตารางเมตรต่อกรัม เมื่อนำเส้นใยไทเทเนียมไดออกไซด์ไปใช้เป็นวัฏภาคนิ่งในโครมาโทกราฟีแบบแผ่นบาง (TLC) สำหรับการแยกสารประกอบที่เป็นเบส ได้แก่ เมทิลไวโอเลต เมทิลลีนบลูไฮเดรต และคอนโกเรด โดยได้เปรียบเทียบกับการใช้อุณหภูมิเป็นวัฏภาคนิ่ง พบว่าเส้นใยไทเทเนียมไดออกไซด์ TLC ให้ประสิทธิภาพในการแยกสารประกอบที่เป็นเบสได้ดีกว่าอุณหภูมิ TLC โดยการวิเคราะห์ในภาวะเบสคาร์ทีทาร์เดชันแพคเตอร์ของเมทิลไวโอเลตและเมทิลลีนบลูไฮเดรตซึ่งมีประจุบวกบนเส้นใยไทเทเนียมไดออกไซด์ TLC มากกว่าคาร์ทีทาร์เดชันแพคเตอร์บนอนุภาคซิลิกา TLC ในขณะที่คอนโกเรดซึ่งมีประจุลบคาร์ทีทาร์เดชันแพคเตอร์บนเส้นใยไทเทเนียมไดออกไซด์ TLC น้อยกว่าคาร์ทีทาร์เดชันแพคเตอร์บนอนุภาคซิลิกา TLC นอกจากนี้เวลาที่ใช้ในการวิเคราะห์ด้วยเส้นใยไทเทเนียมไดออกไซด์ TLC น้อยกว่าการวิเคราะห์ด้วยอนุภาคซิลิกา TLC

สาขาวิชา ปิโตรเคมีและวิทยาศาสตร์พอลิเมอร์ ลายมือชื่อ.....

ปีการศึกษา 2554..... ลายมือชื่อ อ.ที่ปรึกษาวิทยานิพนธ์หลัก.....

ลายมือชื่อ อ.ที่ปรึกษาวิทยานิพนธ์ร่วม.....

# # 5272595523: MAJOR PETROCHEMISTRY AND POLYMER SCIENCE  
KEYWORDS: TITANIA FIBER/ ELECTROSPINNING/ THIN LAYER  
CHROMATOGRAPHY

SUPAMAS KANJANAKUNTHON: PREPARATION OF TITANIUM  
DIOXIDE FIBERS AS STATIONARY PHASE IN THIN LAYER  
CHROMATOGRAPHY. ADVISOR: PUTTARUKSA VARANUSUPAKUL,  
Ph.D., CO-ADVISOR: NIPAKA SUKPIROM, Ph.D., 68 pp.

In this study, the electrospun fibrous titania were prepared via sol-gel process of titanium tetraisopropoxide and fabricated with electrospinning method. The electrospinning factors that affect the fibers morphology were studied. The electric potential, the distance between a needle and a collector, and the flow rate of the solution influenced the fiber size. At higher PVP:TiO<sub>2</sub> ratio, the fiber diameter, the specific surface area and the pore size decreased. When calcination temperature was increased, fiber diameter and specific surface area decreased while the pore size increased and led to transformation of the titania from anatase to rutile. The electrospun fibrous titania had the average diameter range of 50-190 nm and the specific surface area of 2-34 m<sup>2</sup>/g. The electrospun fibrous titania was used as stationary phase in thin layer chromatography for separation of basic dye compounds which were methyl violet, methylene blue hydrate, and congo red, and compared with particulate silica stationary phase. The efficiency of dye separation using the electrospun fibrous titania TLC was better than the particulate silica TLC. In analysis at basic condition, retardation factors of positively charged methyl violet and methylene blue hydrate, on the electrospun fibrous titania TLC were higher than those on the particulate silica TLC. While retardation factor of negatively charged congo red, on the electrospun fibrous titania TLC was lower than that on the particulate silica TLC. In addition, the analysis time of the electrospun fibrous titania TLC was shorter than that of the particulate silica TLC.

Field of study: Petrochemistry and Polymer Science

Academic Year: 2011

Student's Signature.....

Advisor's Signature.....

Co-advisor's Signature.....

## ACKNOWLEDGEMENTS

The author thanks many people for kindly providing the knowledge of this study. First, I would like to express gratitude and appreciation to my advisor, Dr. Puttaruksa Varanusupakul and co-advisor, Dr. Nipaka Sukpirom for generosity, plentiful instruction, continuous assistance, sincere encouragements, kind enduringness for my mistake, and critical proofreading throughout this research. I would like to extend my thanks to Assistant Professor Dr. Warinthorn Chavasiri, Assistant Professor Dr. Varawut Tangpasuthadol at Department of Chemistry, Faculty of Science, Chulalongkorn University and Assistant Professor Dr. Jinda Yenyongchaiwat at Program of Chemistry, Faculty of Science and Technology, Bansomdejchaopraya Rajabhat University.

I would like to thank The Asahi Glass Foundation 2011 Overseas Research Grants for funding this research. This research has been partially supported by National Center of Excellence for Petroleum, Petrochemicals and Advanced Materials (NCE-PPAM).

In addition, I would like to thank many people in Chromatography and Separation Research Unit and all members of 1205/1207 Laboratory. I would like to thank Mr. Taweesak Chanduang for all his assistance in building all equipments.

Finally, I would like to thank my heartfelt gratitude goes to my beloved family; father, mother, my brother, my sister and my intimate friends for all their love, understanding and support.

# CONTENTS

	<b>Page</b>
ABSTRACT IN THAI .....	iv
ABSTRACT IN ENGLISH .....	v
ACKNOWLEDGEMENTS .....	vi
CONTENTS .....	vii
LIST OF TABLES .....	x
LIST OF FIGURES .....	xi
LIST OF SCHEMES .....	xiv
LIST OF ABBREVIATIONS .....	xv
<b>CHAPTER I INTRODUCTION .....</b>	<b>1</b>
1.1 Statement of purpose .....	1
1.2 Objective of this research .....	3
1.3 Scopes of this research .....	3
1.4 The benefit of this research .....	4
<b>CHAPTER II THEORY .....</b>	<b>5</b>
2.1 Electrospinning .....	5
2.1.1 Parameters of electrospinning process .....	6
2.1.1.1 The polymer solution .....	6
2.1.1.2 The processing condition .....	7
2.1.1.2.1 Electric potential .....	7
2.1.1.2.2 Distance between a needle and a collector .....	8
2.1.1.2.3 Flow rate of the solution .....	8
2.1.1.2.4 Diameter of needle .....	9
2.2 Titanium dioxide .....	9
2.2.1 Properties of titania surface .....	10
2.2.2 Preparation of titania via sol-gel process .....	11
2.3 Thin layer chromatography .....	14
2.3.1 Principle of TLC .....	14

	<b>Page</b>
2.3.2 Type of stationary phase .....	15
2.3.3 Type of TLC.....	18
2.3.3.1 Thin layer chromatography (TLC).....	18
2.3.3.2 High-performance thin layer chromatography (HPTLC) ...	19
2.3.3.3 Ultrathin layer chromatography (UTLC).....	19
2.3.3.3.1 Monolithic film.....	19
2.3.3.3.2 Nanostructured films .....	21
2.3.3.3.3 Electrospun stationary phase .....	21
2.3.4 Performance of TLC .....	21
2.4 Nitrogen adsorption-desorption analysis .....	22
2.4.1 Classification of adsorption isotherm .....	23
<b>CHAPTER III EXPERIMENTAL.....</b>	<b>25</b>
3.1 Materials and chemicals.....	25
3.1.1 Preparation of electrospun fibrous titania .....	25
3.1.2 Thin layer chromatography .....	25
3.2 Methodology .....	26
3.2.1 Preparation of electrospun fibrous titania .....	26
3.2.2 Characterization of electrospun titania fibers .....	27
3.2.2.1 Morphology of as-spun fibers and electrospun fibrous titania .....	27
3.2.2.2 Crystalline structure of the electrospun fibrous titania .....	28
3.2.2.3 Nitrogen adsorption-desorption analysis .....	28
3.2.3 Thin layer chromatography.....	28
<b>CHAPTER IV RESULTS AND DISCUSSION .....</b>	<b>30</b>
4.1 Morphology of electrospun fibrous titania .....	31
4.2 Crystalline structure of the electrospun fibrous titania .....	39
4.3 Nitrogen adsorption-desorption analysis .....	41
4.4 Effect of the collectors .....	51
4.5 Thin layer chromatography.....	52



	<b>Page</b>
4.5.1 Mobile phase transport.....	54
4.5.2 Separation of dyes.....	56
<b>CHAPTER V CONCLUSION.....</b>	<b>61</b>
<b>REFERENCES.....</b>	<b>63</b>
<b>VITA.....</b>	<b>68</b>

## LIST OF TABLES

<b>Table</b>		<b>Page</b>
2.1	Types of stationary phase and supports .....	16
2.2	Pore features of adsorption isotherm.....	23
2.3	IUPAC classification of pores.....	24
3.1	Compositions of polymer solutions and PVP:TiO <sub>2</sub> ratios .....	26
3.2	Conditions of TLC separations .....	29
4.1	Average diameters of the as-spun fibers and the electrospun fibrous titania at the calcination temperature of 450°C for 3h.....	34
4.2	Average diameters of the as-spun fibers and the electrospun fibrous titania at various PVP:TiO <sub>2</sub> ratios (by weight).....	36
4.3	Average diameters of the electrospun fibrous titania at various calcination temperatures for 3 h.....	38
4.4	Specific surface area, monolayer volume and average pore diameter of the electrospun fibrous titania at various conditions .....	46
4.5	Specific surface area, monolayer volume and average pore diameter of the electrospun fibrous titania at various PVP:TiO <sub>2</sub> ratios.....	49
4.6	Specific surface area, monolayer volume and average pore diameter of the electrospun fibrous titania at various calcination temperatures .....	51
4.7	Electrospinning conditions for preparation of the electrospun fibrous titania stationary phase.....	53
4.8	Comparison of $\kappa$ values .....	55
4.9	Spot width, retardation factor ( $R_f$ ) and plate height ( $H$ ) of dye compounds (n=2) for various conditions of the electrospun fibrous titania and the particulate silica TLC .....	58

## LIST OF FIGURES

Figure		Page
2.1	Schematics of electrospinning set up apparatus: (a) a typical horizontal and (b) a typical vertical .....	6
2.2	Unit cells of (a) brookite, (b) anatase and (c) rutile .....	10
2.3	Crystalline structures of (a) brookite, (b) anatase and (c) rutile ...	10
2.4	Thin layer plate development.....	14
2.5	The IUPAC classification of adsorption isotherm .....	23
4.1	The IR spectra of the fibers of (a) PVP fibers and (b) the as-spun fibers .....	31
4.2	SEM images of the as-spun fibers at various conditions of the flow rate of the solution, the electric potential and the distance between a needle and a collector. The original magnification of 10,000x.....	32
4.3	SEM images of the electrospun fibrous titania at various conditions of the flow rate of the solution, the electric potential and the distance between a needle and a collector. The fibers were calcined at 450°C for 3 h. The original magnification of 10,000x.....	33
4.4	SEM images of the electrospun fibers at various PVP:TiO <sub>2</sub> ratios (by weight). The original magnification of 10,000x (the flow rate of 15 μL/min, the electric potential of 25 kV, the distance between a needle and a collector of 15 cm and the calcination temperature of 450°C for 3 h).....	36
4.5	TEM images of the electrospun fibrous titania with PVP:TiO <sub>2</sub> ratios of (a) 1:2, (b) 1:1 and (c) 2:1 by weight.....	37

<b>Figure</b>		<b>Page</b>
4.6	SEM images of the electrospun fibrous titania at various calcination temperatures. The original magnifications of 10,000x (the flow rate of 15 $\mu$ L/min, the electric potential of 25 kV, the distance between a needle and a collector of 15 cm and the PVP:TiO <sub>2</sub> ratio of 1:1 by weight).....	38
4.7	TEM images of electrospun fibrous titania with calcination temperatures of (a) 450°C, (b) 500°C and (c) 550°C for 3 h.....	39
4.8	XRD patterns of the electrospun fibrous titania with PVP:TiO <sub>2</sub> ratios of (a) 1:2, (b) 1:1 and (c) 2:1 by weight.....	39
4.9	XRD patterns of (a) the as-spun fibers and the electrospun fibrous titania after calcination at (b) 450°C, (c) 500°C and (d) 550°C for 3 h.....	40
4.10	Nitrogen adsorption-desorption isotherms of the electrospun fibrous titania at various conditions of the flow rate of the solution, the electric potential and the distance between a needle and a collector. The fibers were calcined at 450°C for 3 h.....	43
4.11	BET-Plots of the electrospun fibrous titania at various conditions of the flow rate of the solution, the electric potential and the distance between a needle and a collector. The fibers were calcined at 450°C for 3 h.....	44
4.12	Pore size distribution of the electrospun fibrous titania at various conditions of the flow rate of the solution, the electric potential and the distance between a needle and a collector. The fibers were calcined at 450°C for 3 h.....	45
4.13	Characteristics of the electrospun fibrous titania at various PVP:TiO <sub>2</sub> ratios: (a) nitrogen adsorption-desorption isotherms, (b) BET-Plots and (c) pore size distributions.....	48
4.14	Characteristics of the electrospun fibrous titania at various calcination temperatures: (a) nitrogen adsorption-desorption isotherms, (b) BET-Plots and (c) pore size distributions.....	50

<b>Figure</b>		<b>Page</b>
4.15	SEM image of the cross section of spin-coated layer .....	52
4.16	SEM image of the cross section of electrospun fibrous titania at the flow rate of 15 $\mu$ L/min, the electric potential of 25 kV, the distance between a needle and a collector of 15 cm, the PVP:TiO <sub>2</sub> ratio of 1:1 by weight, the calcination temperature of 450°C and the electrospinning time of 1 h.....	53
4.17	Mobile phase migration distances versus developing time on particulate silica and electrospun fibrous titania TLC plates .....	55
4.18	The molecular structure of methyl violet, methylene blue hydrate and congo red .....	56
4.19	The separation of dye compounds on (1-5) the electrospun fibrous titania TLC from various conditions as shown in Table 4.7 and (6) the particulate silica TLC.....	57

## LIST OF SCHEMES

<b>Scheme</b>		<b>Page</b>
4.1	Hydrolysis of TTiP.....	30
4.2	The expected reaction pathway of TTiP and acetic acid.....	30

## LIST OF ABBREVIATIONS

%v	Percentage by volume
%v/v	Percentage of volume by volume
%wt	Percentage by weight
°C	Celcius degree
μL	Microliter
μm	Micrometer
cm	Centimeter
cm <sup>2</sup>	Square centimeter
g	Gram
h	Hour
kV	Kilovolt
M	Molar concentration
m <sup>2</sup>	Square meter
min	Minute
mL	Milliliter
mm	Millimeter
nm	Nanometer
PVP	Polyvinylpyrrolidone
rpm	Round per minute
sec	Second
TTiP	Titanium tetraisopropoxide

# CHAPTER I

## INTRODUCTION

### 1.1 Statement of purpose

Thin layer chromatography (TLC) is a planar chromatography technique that is used in monitoring a chemical reaction and testing the purity of samples. The advantages of TLC technique include simple equipment, low cost and rapid identification of components in sample. In addition, the simultaneous analysis of samples and standard substances can be achieved in a single run. A stationary phase for TLC is normally solid stationary phase particles that are coated on a support plate, usually glass or aluminum. A binder is sometimes added to bind the solid particles on the plate. At present, TLC was developed and so called high-performance TLC (HPTLC) and ultrathin layer chromatography (UTLC). In HPTLC, a particle size and a thickness of stationary phase were reduced. The particle size is about 5-7  $\mu\text{m}$  with a thickness of 150-200  $\mu\text{m}$ . UTLC, a new categorized of TLC, was developed to further improve sensitivity and reduce amount of consumables required for TLC [1-2]. Its advantages include decreasing of analysis time and sample volume. UTLC have been applied for various application such as amino acids, pesticides, steroids, active ingredients in pharmaceuticals, phenols, plasticisers, lipophilic dyestuffs and flavanols [3]. Nowadays, UTLC plates were a monolithic silica gel fabricated via glancing-angle deposition (GLAD). For example, Bezuidenhout and Brett [4] produced UTLC plates with controllable nanostructure and thickness and show the layer separation characteristics depends on the film nanostructure. Moreover, a monolithic silica gel with 10  $\mu\text{m}$  thickness is commercially available from Merck (Germany). However, this fabrication technique is complicated. Recently, a new technique for UTLC plate fabrication was reported using an electrospinning method which is quickly and inexpensively [5-6]. Electrospinning process was performed by



pumping a polymer solution while applying the electric potential across the syringe needle and the collector which normally an aluminum foil substrate. The technique results in the fibers with tunable diameters and mat thicknesses. The electrospun nanofibrous stationary phase offers a large surface area and uniformity which can decrease the band dispersion in TLC. Also, the binder is not necessitated for attaching the fibers onto the support plate. Clark and Olesik [5] reported the preparation of polyacrylonitrile (PAN) stationary phases via electrospinning and used in UTLC. The components were completely separated in a short time and used lower quantity of solvent than using in commercial TLC. Moreover, they prepared the glassy carbon stationary phase with electrospinning method and compared with electrospun PAN UTLC and commercial silica TLC [6]. In addition, the mobile phase can transport faster in the electrospun PAN and glassy carbon UTLC than in commercial silica TLC which indicated the reduction of analysis time using electrospun UTLC plates.

Silica is commonly used as the stationary phase in TLC but a main weakness of silica stationary phase is a poor separation of basic compounds. Titania or titanium dioxide is an interested alternation stationary phase because of high selectivity for basic compound and isomer, and also can be stably used in wide range of pH value [7-8]. Winkler and Marmé [8] compared the separation efficiency of nine different pyridine and aniline derivatives on titania, silica, zirconia and alumina column in normal-phase liquid chromatography and found that only titania column can separate all of the mixture. Silica, zirconia and alumina column cannot completely separate components of the mixture even though using gradient conditions.

Titania nanofibers can be synthesized by sol-gel method combined with electrospinning. Fabrication of titania nanofibers were mixed with organic polymers such as polyvinylpyrrolidone (PVP), polyvinyl alcohol (PVA) and polyvinyl acetate (PVAc) [9-16]. The viscosity of polymer solution and porosity of nanofibers after calcination can be increased by adding these polymers. Generally, titanium tetrabutoxide (TiBU) and titanium tetraisopropoxide (TTiP) were used as titania precursor [9-16]. Li and Xia [14] fabricated titania nanofibers by using TTiP and PVP as precursor. The increasing of concentration of PVP, TTiP and flow rate of the solution affected the diameter of nanofibers. Moreover, the average diameter was

slightly increased with increasing an electric potential. Chuangchote et al. [11] reported a simple procedure for the fabrication of titania nanofibers by the combination of electrospinning and sol-gel techniques by using PVP, TiBU and acetylacetone in methanol. Acetylacetone was used to slow down the hydrolysis and the condensation reactions for prevention of breakage of fibers during those reactions. Moreover, the increasing of calcination temperature resulted in smaller nanofibers but a larger size of titania crystallites and the form of anatase and rutile phase of titania was varied upon the calcination temperature. The flexible titania nanofibers were developed by Park, et al. [16] to improve the brittle of titania nanofibers with electrospinning after calcination. The mechanical properties and flexibility of nanofibers were better than previous researches. Therefore, this research has an interested in benefits of titania nanofibers fabricated by electrospinning method for use as the stationary phase in TLC.

## **1.2 Objective of this research**

The aims of the research are focused on fabrication of titania nanofibers by electrospinning technique and studying of factors which affect separation performance of titania nanofibrous stationary phase.

## **1.3 Scopes of this research**

- 1.3.1 Fabrication of titania nanofibrous stationary phase by electrospinning.
- 1.3.2 Examining the efficiency of titania nanofibrous as a stationary phase in TLC.
- 1.3.3 Comparing the separation performance of titania nanofibrous stationary phase with commercial silica TLC plates.

#### **1.4 The benefit of this research**

The titania nanofibers achieved from electrospinning can be used as stationary phase in TLC which can be useful in the separation of basic compounds.

## **CHAPTER II**

### **THEORY**

#### **2.1 Electrospinning**

Electrostatic spinning or electrospinning is a process that creates fibers with diameter of micro or nanometer ranges through electrically charged jet of polymer solution or polymer melt. Advantages of the electrospinning are an ability to produce small diameter and good mechanical properties of the fibers. It leads to fibers with high surface area to volume ratio. Moreover, the electrospinning can control fiber morphology such as size, shape and porosity. There are a number of potential applications for the fibers including chemical and optical sensors, electrode materials, protective clothing, biomedical, pharmaceutical, healthcare, tissue engineering scaffolds, separation membranes, wound dressing materials and catalyst, etc.

The minimum equipment requirements for electrospinning process consist of a viscous polymer solution or melt can be carried out either vertically or horizontally, depending on the direction of normal line between needle and collector, a pipette tip or syringe used as reservoir with metal needle, a high voltage power supply and a grounded collecting plate such as a metal screen, and rotation drum or mandrel. The electrospinning set up is shown in Fig. 2.1.

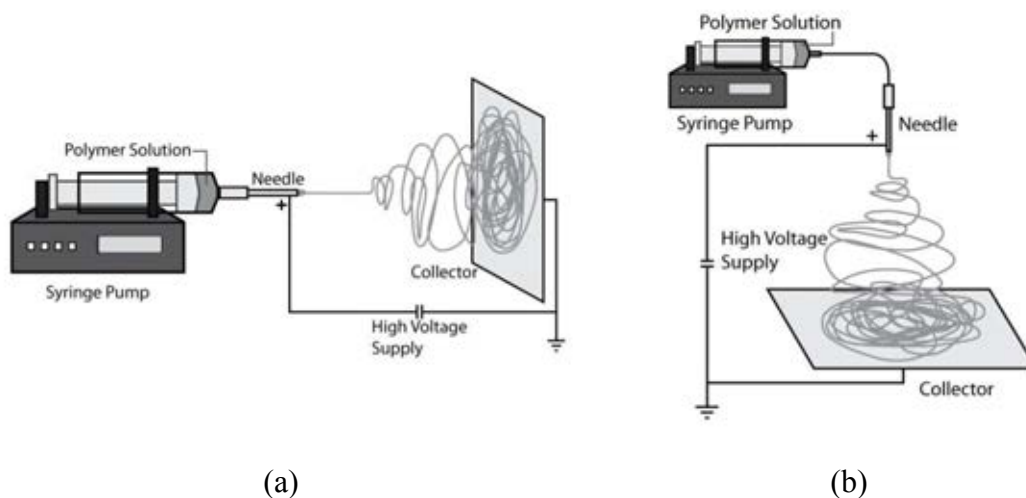


**Figure 2.1** Schematics of electrospinning set up apparatus: (a) a typical horizontal and (b) a typical vertical.

The high voltage is applied to the needle which connected with the polymer reservoir that charges are induced within the fluid. When the charges within the fluid overcome the surface tension, the fluid jet will erupt from droplet of the polymer solution at the tip of the needle resulting into conical shape, referred to as Taylor cone. The jet stretches toward the grounded collector.

### 2.1.1 Parameters of electrospinning process

There are many parameters that affect the morphology of the electrospun fibers. The parameters can be classified into polymer solution and processing condition.

#### 2.1.1.1 The polymer solution

The properties of the polymer solution such as viscosity, surface tension, solution conductivity and dielectric effect of solvent have the influence in the morphological appearance and diameter of the electrospun fibers. The viscosity of the solution affect the elongation of the solution that has an effect on the diameter of the resultant electrospun fibers [17-18].

Viscosity of the polymer solution depends on molecular weight and concentration of the polymer. Generally, high molecular weight and concentration of the polymer give high viscosity of the polymer solution. Changing of the viscosity affects the fiber morphology and diameter. Deitzel et al. [19] reported concentration of PEO/water solution below 4 %wt, the fibers and droplets appeared. The concentration higher than 10 %wt made the control of the solution flow rate to the tip unstable. Moreover, they studied the concentration range of 4-10 %wt. At the low concentration, the result showed an irregular, undulating morphology with large variation in diameter along a single fiber. At the high concentration, the fibers are regular, larger diameter and more uniform.

Chuangchote et al. [20] reported the effect of molecular weight at high concentration. The electrospinning of the lower molecular weight of polyvinylpyrrolidone (PVP) resulted in more twisted and flat fiber structures than the electrospinning of higher molecular weight of PVP. It dues to a charge jet from the low molecular weight could be stretched during bending instability more than that from the high molecular weight.

### **2.1.1.2 The processing condition**

#### **2.1.1.2.1 Electric potential**

An important parameter of electrospinning is the electric potential or voltage to polymer solution. The electric potential provides the surface charge on the electrospinning jet and influenced on diameter and morphology of the fibers. When the electric potential was increased, the polymer jet was discharged with a greater electrostatic repulsion force on the jet, results in a thinner fiber formation.

Lee et al. [21] controlled the morphology of titania nanofibers by applied voltage. Their result showed that the controlled electric potential was the significant factor that determined the morphology of the electrospun.

Increasing the electric potential make rising of the electrostatic repulsion force between a needle and a collector resulted in the smaller diameter.

The electric potential relates to the diameter fiber, the distance between a needle and a collector and the concentration of the polymer solution are considerably parameters affecting on the morphology and size of the fibers.

#### **2.1.1.2.2 Distance between a needle and a collector**

The distance from a needle to a collector has an influence on electric potential strength and jet flight time. Decreasing in the distance shortens solvent evaporation time and flight time but increases the electric potential strength. Chowdhury and Stylios [22] studied the effect of the distance from a needle to a collector. They reported that increasing the gap, the electrospun are dried and fully stretched so the fiber diameter is reduced. It due to the wider gap allowed more time for the fluid jet to stretch and for the solvent to completely evaporation.

#### **2.1.1.2.3 Flow rate of the solution**

Flow rate of the solution is the rate at which the polymer solution is pumped into the needle tip. The flow rate affect on the rate of solvent evaporation from the needle which influence on the fiber morphology. Jeun et al. [23] reported the effect of the flow rate on fiber diameter. At lower flow rate, the fibers were fine and a narrow distribution of the fiber diameters was observed. Increasing the flow rate, the fiber beads were formed and showed a broad distribution of the fiber diameters. When the flow rate exceeded a critical value, unstable jet and beads of the fiber were formed. It was the result of the delivery rate of the solution jet to the needle exceeded the rate at which the solution was removed from the needle by electric potential.

#### **2.1.1.2.4 Diameter of needle**

The internal diameter of the needle affects the fiber morphology. Biber et al. [24] reported the mean diameter slightly increases by increasing the needle diameter. With the small needle diameter, the flatter fibers are formed and bead formation are reduced due to the acceleration of jet decreases and this allows more time for the polymer solution to be stretched and elongated before it was collected. However, if the needle diameter is too small, it may not be possible to eject a solution droplet at the needle tip. With the large needle diameter, the fiber morphology is big and has bead formation.

## **2.2 Titanium dioxide**

Titanium dioxide ( $\text{TiO}_2$ ) or titania has a wide range of applications such as a white pigment in paints and cosmetic product, a corrosion-protective coatings, an optical coating, a photocatalyst, catalyst support and electronics. Moreover, it plays an important role in the biocompatibility of bone implants. Titania has naturally three important crystalline forms of brookite, anatase and rutile. But only anatase and rutile are commercial value and play any role in the applications.

Brookite is the least common of the three forms. It has an orthorhombic crystal structure. Its mechanical properties are very similar to those of rutile.

The commercial phase of titania is anatase. It has a tetragonal crystal structure, in which the Ti–O octahedral share four corners [25].

Rutile is a stable form of titania. At high temperature, the other forms can be transformed to rutile. It has a crystal structure similar to anatase, but the octahedra share four edges instead of four corners [25].



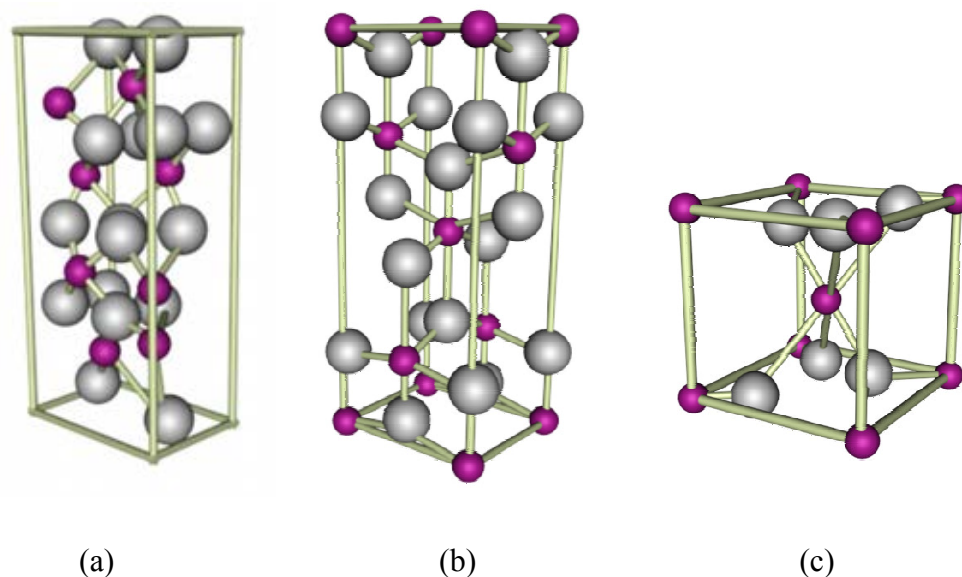


**Figure 2.2** Unit cells of (a) brookite, (b) anatase and (c) rutile. Grey and red spheres represent oxygen and titanium, respectively [26].

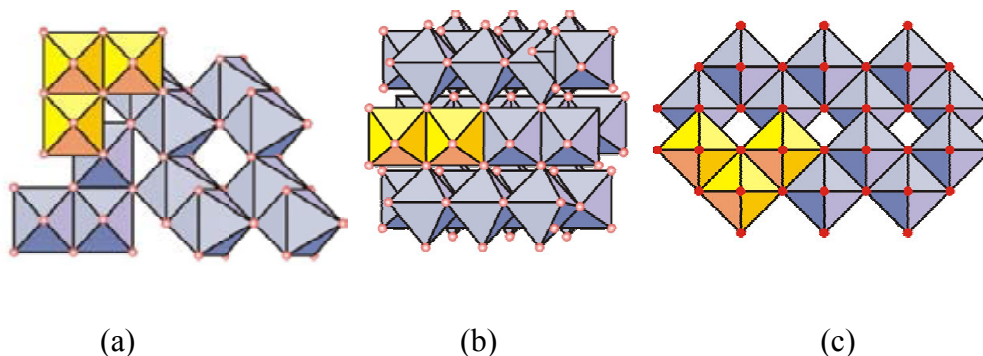


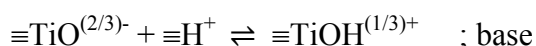
**Figure 2.3** Crystalline structures of (a) brookite, (b) anatase and (c) rutile [26].

### 2.2.1 Properties of titania surface

The metal oxide surface contains hydroxyl ( $-\text{OH}$ ) group as  $\text{M}-\text{OH}$ . Properties of metal oxide depend on the terminating hydroxyl group on their surfaces which are governed by the charge distribution between the metal, oxygen and hydrogen atom. Three different cases may be identified (a)  $\text{M}^{\delta+} \text{OH}^{\delta-}$ ; (b)  $\text{M}-\text{O}-\text{H}$  and (c)  $\text{MO}^{\delta-} \text{H}^{\delta+}$ . Structure (a) depicts the situation of an M atom with low electron

affinity, (b) an intermediate situation leading to a covalent bond along the M–O–H group and (c) the case for an M atom with a high electron drawing potential [8].

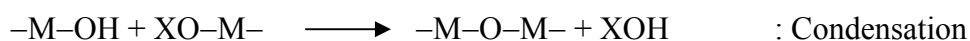
The isoelectric point ( $pI$ ) of silica is about 1-2 [8, 27-28]. It shows an acidic surface like case (c). For alumina, the  $pI$  is about 7-9 [8, 28-29], it shows a basic surface like case (a). On the other hand, the  $pI$  of the titania is range of 3-6 [8, 27-30], it lies in between acidic and basic. The titania surface differ in partial positive charge and the acid-base character of these sites is represented by the following surface equilibria [7]:



Various synthesis methods such as hydrothermal synthesis, microemulsion, solvothermal, electrodeposition, sonochemical and sol-gel have been used to prepare the titania. Sol-gel is a good method to synthesize metallic oxide.

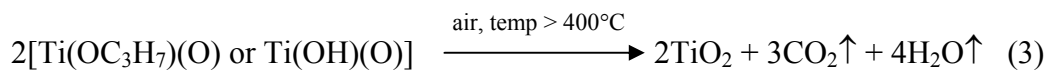
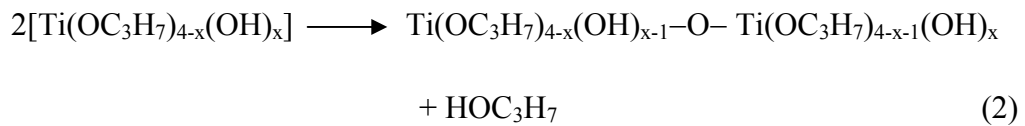
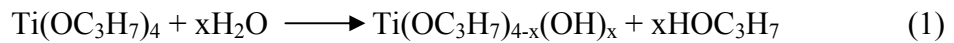
### 2.2.2 Preparation of titania via sol-gel process

In sol-gel process, inorganic metal salts or metal organic compounds such as metal alkoxides is usually used as a precursor. Titania precursor is widely prepared by hydrolysis and polycondensation reactions of titanium alkoxide  $[\text{Ti}(\text{OR})_n]$  to form an oxide network. The reaction is written as follow:



Where; X is R (an alkyl group) or H.

There are many researchers investigated to prepare titania via the sol-gel process such as Jorge et al. [31] described the preparation of titania reaction which titanium tetraisopropoxide (TTiP) was used as a reactant. The first step is the hydrolysis of the TTiP as in (1). The second step is the condensation of the hydrolyzed product, with the bridging of oxygens. The reaction was given in (2). The final material before calcination was  $\text{Ti}(\text{OC}_3\text{H}_7)_{2-y}(\text{O})_y$  or  $\text{Ti}(\text{OH})_{2-y}(\text{O})_y$ ,  $y$  can be 1 or 2, every titanium atom was formed part of the network. After calcination, every oxygen was bonded with titanium atom and pure homogeneous oxide network (titania) was obtained as in (3).



Ali et al. [32] prepared titania nano-powder by using TTiP as a precursor via sol-gel method in acidic condition. The grain size of nano-titania powder was 25 nm and it increased with increasing of the calcination temperature. The phase transformation of nano-titania from anatase to rutile occurred at 900°C.

Ki and Hee [33] introduced a particle preparation method which can decrease the particle size. The method consisted of a semibatch-batch two stage reaction. First stage is a semibatch process and second stage is a batch process. They reported the titania particle size grew to 132 nm in first stage and decreased about 42 nm in second stage. As a result, it can be concluded that the particle prepared by using the two stage reaction had a smaller particle size than those obtain from the single stage process.

The ultrasonic irradiation from outside a reactor (bath-US) was applied during the preparation of titania [34]. They reported it had a similar effect on titania particle properties as ultrasonic irradiation inside a reactor with a probe tip (tip-US). Comparing of titania preparation by bath-US and tip-US, titania which was prepared by the tip-US was smaller particle size and higher surface area than the titania which was prepared by the bath-US but less pore volume that affect on reactivity for the degradation of 4-chlorophenol.

The effect of calcination temperature is one of important factors that affect titania properties. Su et al. [35] prepared titania powder for using as photocatalyst in decomposition of salicylic acid. The titania was prepared by hydrolysis and polycondensation of titanium tetrabutoxide which was used as a precursor in isopropanol. They reported the stable sol can be obtained at  $\text{pH} < 2$ . After heat treatment, anatase grew first. Increasing the calcination temperature induced phase transformation from anatase to rutile. Moreover, an increasing of the temperature is associated with the increase in the particle size but decrease in a specific surface area of the titania.

Sayilkan et al. [36] investigated effect of the calcination temperature and hydrolysis catalyst on the properties of titania prepared by the sol-gel process. The titania can be synthesized in the absence of the catalyst but the anatase phase was formed at high temperature ( $400^{\circ}\text{C}$ ) and it has a micro-, meso- and macropores. The catalyst had an importance in the reaction. It was found the formation of the anatase phase of titania at low temperature ( $200\text{-}300^{\circ}\text{C}$ ).

Li et al. [37] studied the influence of preparation parameters on the microstructure of titania powders which was prepared via sol-gel method. They concluded that the anatase particle size can be controlled by adjusting the aging time of the dry gel. The rutile amount can be controlled by adjusting the wet gel aging time.

## 2.3 Thin layer chromatography

### 2.3.1 Principle of TLC

Thin layer chromatography (TLC) is a separation process which the stationary phase or sorbent was fixed on a solid substrate or support. The common supports are a glass plate, aluminum and plastic sheet. The TLC can be used to monitor the progress of a reaction, determine the purity of a substance and indentify compounds present in a given substance. The TLC has a number of advantages including ease of use, high sensitivity, speed of separation, wide application to a great number of different samples and relatively low cost [38].

The process involves develop chamber, the mobile phase (solvent), the stationary phase (sorbent) and sample molecules.

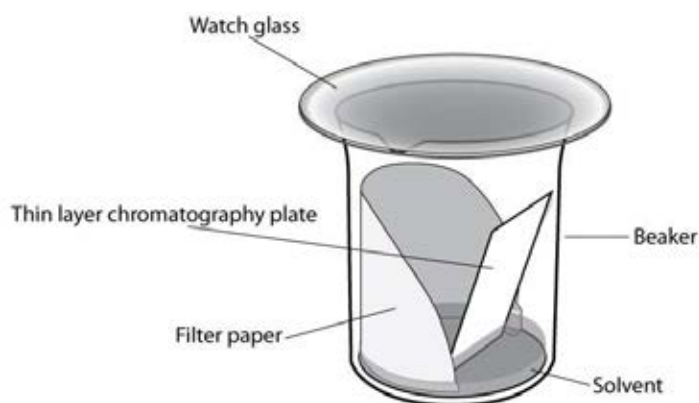


**Figure 2.4** Thin layer plate development.

The common developing chamber is glass beaker covered with watch glass. To ensure the air space in the developing chamber is saturated with the mobile phase, the inner wall is normally lined with filter paper and wait several minutes. Be

careful that the paper is not so high that it prevents proper seating of the lid on the tank.

The mobile phase system is the factor with influence on the TLC. It performs to dissolve the mixture of substances, transport the substances to be separated across the stationary phase layer and provide adequate selectivity for the substance mixture to be separated. The mobile phase should be adequate purity and stability, low viscosity, linear partition isotherm, low toxicity and suitable vapor pressure [39].

The components of mobile phase are mixed thoroughly in a mixing cylinder, Erlenmeyer flask, or other container before adding them to the developing chamber. Most mobile phase proportions are measured by volume. It is convenient to pour the mixed mobile phase over the lining paper as it is poured into the developing chamber. This will speed the saturation of the paper and the chamber. This is usually done about an hour before the plates are to be developed [38].

There are various substances for using as stationary phase, including aluminum oxides, aluminum silicates, calcium carbonate, kieselguhr, magnesium oxide, polyamides, silica gel, chemically modified silica gel, and mixed layers of two or more materials. Silica gel is the most widely used as stationary phase and the normal phase mode with organic mobile phase.

### **2.3.2 Type of stationary phase**

The most important types of stationary phase used in proprietary products for TLC are listed in Table 2.1 in alphabetical order with the corresponding supports.

**Table 2.1** Types of stationary phase and supports [39].

<b>Stationary phase material</b>	<b>Support</b>
Aluminum oxide 60,150	Aluminum foil, glass plate, plastic film
Cellulose (unmodified)	Aluminum foil, glass plate, plastic film
Cellulose (acetylated)	Glass plate, plastic sheet
PEI-Cellulose	Glass plate, plastic sheet
Silica gel 40	Glass plate
Silica gel 60	Aluminum foil, glass plate, plastic film
Kieselguhr	Aluminum foil, glass plate
LiChrospher® Si 60	Glass plate
Si 50000	Glass plate
Si 60 RAMAN	Aluminum foil
<b>Silica gel, modified:</b>	
CHIR (chiral)	Glass plate
CN (cyano)	Glass plate
DIOL	Glass plate
NH <sub>2</sub> (amino)	Aluminum foil, glass plate
Silica gel 60 caffeine-impregnated	Glass plate
Silical G ammonium sulfate- impregnated	Glass plate
Silica gel 60 silanized (RP-2), RP-8	Glass plate
RP-18	Aluminum foil, glass plate
<b>Mixed layers:</b>	
Aluminum oxide/acetylated cellulose	Glass plate
Cellulose/silica	Glass plate
Cellulose 300 DEAE/cellulose 300 HR	Glass plate
Silica gel 60/ kieselguhr	Aluminum foil, glass plate

Silica gel is the most widely used layer material for TLC. Separations take place primarily by hydrogen bonding or dipole interaction with surface silanol groups by using lipophilic mobile phases, and analytes are separated into groups according to their polarity.

Other TLC stationary phase include aluminum oxide or alumina, magnesium oxide, polyamide, and kieselguhr.

Alumina is a polar stationary phase that is similar to silica gel in its general chromatographic properties, but it has an especially high adsorption affinity

for carbon-carbon double bonds and better selectivity toward aromatic hydrocarbons and their derivatives.

Both of silica gel and alumina are inorganic substances that are used chiefly to separate lipophilic compounds or those soluble mainly in organic solvents. Cellulose is mainly used to separate hydrophilic compounds such as sugars, amino acids inorganic ions, and nucleic acid derivatives. The separation process occurring on cellulose is mainly that of partition because the adsorbed water molecules cover the cellulose molecules, being joined to them by hydrogen bonds.

Polyamides have surface  $-\text{CO}-\text{NH}-$  groups and show high affinity and selectivity for polar compounds that can form hydrogen bonds with exposed carbonyl groups. The separation depends on the strength of the hydrogen bonds formed between the polyamide molecules and the substances being separated [40].

There are other stationary phase are used in chromatography but have not used in TLC such as zirconia and titania.

Zirconia or  $\text{ZrO}_2$  has a high thermal and chemical stability over a wide range of temperature (up to  $200^\circ\text{C}$ ) and pH (1 to 14), different selectivity, similar effectiveness to silica stationary phase and commercial availability [41].

Titania surface offers enhanced column long-term stability and can withstand adverse conditions of pH between 1 and 14 and temperature up to  $150^\circ\text{C}$ . Moreover, the surface of titania can exhibit mixed-mode interactions involving essentially ligand-exchange on Lewis acid sites and weak anion or cation exchange on Brønsted groups depending on the pH of the medium, according to the surface isoelectric point of the material [42].

Grün et al. [43] reported the behavior of silica, alumina, titania, zirconia and aluminosilicate stationary phase in normal-phase high-performance liquid chromatography. When separation basic compound on the alumina, zirconia and titania stationary phase, the results showed short retention times and symmetrical peaks. In contrast to those oxides, the silica stationary phase exhibits acid properties due to its silanol groups resulting in long retention times and poorly shaped peaks.



Separation acid compound, the silica show symmetrical peaks due to the Brønsted acidity of the silanol groups, whereas the alumina, zirconia and titania showed long retention times and poorly shaped peaks. The behavior of the alumina, zirconia and titania towards polycyclic aromatic hydrocarbons which is neutral compound is determined by their strong Lewis acidity. A stepwise increase of Lewis acidity from alumina to zirconia is reflected by the increasing retention times. But silica shows almost no retention due to the lack of Lewis acid sites. The aluminosilicate is able to separate all types of analytes within acceptable retention times and good peak shapes.

### **2.3.3 Type of TLC**

#### **2.3.3.1 Thin layer chromatography (TLC)**

Today TLC has increasing importance as the separation technique. The applicability of TLC was enhanced by the development of new stationary phase and support.

The stationary phase used most often in TLC is 60 Å silica gel (mean pore diameter 60 Å = 6 nm). About 80% of all TLC separations are performed with this separation medium. Additionally, there are other stationary phases available on TLC and to name a few: bonded phase silica gels (C18, amino, diol), aluminum oxide, cellulose and more.

The particle size distribution and the thickness of the layer are important for distinguishing high quality and highly reproducible TLC plates. For standard silica TLC plates, the particle size distribution is typically between 5-17 µm. The most common thickness of a stationary phase layer is 250 µm for analytical plates [38].

### **2.3.3.2 High-performance thin layer chromatography (HPTLC)**

HPTLC which is the developed TLC has two types of silica gel with 60 Å pores, one is irregular particle and another is spherical particle. The HPTLC stationary phase was smaller than TLC stationary phase that made the HPTLC has advantage over the TLC such as reducing analysis time and the amount of solvent required. Comparison between irregular particle and spherical particle of HPTLC stationary phase, the spherical particle is more rapid separations (about 20% faster) and more compact spots compared to HPTLC plates made with irregular particles. And the spherical allows a tenfold increase in signal intensity compared to a similar layer made with irregular.

### **2.3.3.3 Ultrathin layer chromatography (UTLC)**

The first commercial UTLC with monolithic silica using as stationary phase was introduced by Merck (Germany). The UTLC plates carry a monolithic layer with 10 µm thickness. Nowadays, there are three types of UTLC stationary phase that are monolithic film, nanostructured films and electrospun.

#### **2.3.3.3.1 Monolithic film**

Hauck and Schulz [44] gave the impression of behavior of the UTLC silica gel plates. They tested the separation of pharmaceutically active ingredients, phenols, plasticizers and steroids. The result can be deduced that the UTLC show similar behavior of retention and selectivity properties compared with conventional TLC and HPTLC. They reported the advantage of the UTLC such as absence of binders, reduction of migration distance, migration times and solvent consumption.

Vovk et al. [3] investigated the use of UTLC plates. They compared the separation power of TLC and UTLC. The stationary phase of TLC is the silica gel 60 (thickness of 250 µm) and for UTLC is monolithic silica gel

(thickness of 10  $\mu\text{m}$ ). The UTLC required sample volume of 0.02-0.10  $\mu\text{L}$ , developing distance of 28 mm and migration time of 6.5 min while TLC require 1  $\mu\text{L}$ , 90 mm and 30 min for sample volume, developing distance and migration time, respectively. These results can be concluded TLC required more developing distance, application volume and position. Moreover, it used longer migration time than UTLC. They reported the problems with the application of small volumes (0.02-0.1  $\mu\text{L}$ ) of the analytes were associated mainly with the thickness and the size of the UTLC plates; when applying the samples on these plates with automatic TLC sampler ATS 4, this inconvenience was overcome by fixation of the UTLC plate with additional TLC plates. For a successful evaluation of the compounds on the UTLC plates it was necessary to solve several technical problems concerning the application, development and detection.

Bakry et al. [45] prepared monolithic porous polymer layer for the separation of peptides and proteins. They reported the layer of porous polymer monolith conveniently obtain by photopolymerization can use for the separation of small molecules, peptides, and proteins. For peptides separation, trifluoroacetic acid (TFA) in acetonitrile-water mixture was used as the mobile phase. The location of the separated peptide was detected using a UV lamp. The results showed a good separation of all three spotted peptides with  $R_f$  values of 0.52, 0.41 and 0.30 for angiotensin II, angiotensin II, and neurotensin, respectively. The monolithic TLC performance for separation of protein was tested using a protein mixture containing insulin, cytochrom *c*, lyzosome, and myoglobin which were labeled with fluorescamine before spotting on the plates. The best mobile phase system for the separation included 0.1% TFA in 55 %v aqueous acetonitrile. The developed plates were scanned by fluorodensitometer at 360 nm. The  $R_f$  values of insulin, cytochrom *c*, lyzosome, and myoglobin were 0.836, 0.362, 0.286, and 0.205, respectively.

### 2.3.3.3.2 Nanostructured films

Bezuidenhout and Brett [4] prepared nanostructured UTLC plates by using glancing-angle deposition (GLAD) technique. The plates were made by depositing silica on square glass substrates by electron-beam evaporation in a custom-made ultra-high vacuum chamber. They showed the separation Fast Green FCF, Rhodamine B, Bismark Brown Y, and Sudan IV. The results showed the dye separations successfully performed on the plates. But the thinner films required longer developing times, due to lower mobile phase velocities.

### 2.3.3.3.3 Electrospun stationary phase

Recently, there are using fibers as the stationary phase. Clark and Olesik [5-6] prepared polyacrylonitrile (PAN) and glassy carbon UTLC stationary phases using electrospinning technique. The layers are stable for use without the need for a binder. The thickness of PAN and glassy carbon layers were 25 and 13-16  $\mu\text{m}$ , respectively. The plate height values less than 10  $\mu\text{m}$  over migration distance of 1-6 cm were observed. The weakness points of the plates are low sample capacity, low specific surface area of the fibers (for PAN fibers) and difficulty in optical detection. The good point of the plates was higher mobile phase velocity compared with TLC and HPTLC which can be reduced the migration time of UTLC.

## 2.3.4 Performance of TLC

The retardation factor,  $R_f$ , is a convenient way to express the position of a substance on a developed chromatogram [38]. It is calculated using eq. 2.1.

$$R_f = \frac{Z_s}{Z_f} \quad \dots\text{eq. 2.1}$$

Where;

$Z_s$  is the distance traveled by the analyte front, and

$Z_f$  is the distance traveled by the mobile phase front.

The  $R_f$  values are between 0 and 1, and without units. Distance is measured to the center of the sample zone or spot. If reproducible, the  $R_f$  value should be obtained it is, however, several parameters such as chamber saturation, mobile phase composition, temperature etc. are controlled.

The number of theoretical plate or plate number,  $N$ , is calculated using eq. 2.2.

$$N = 16 \left( \frac{R_f Z_f}{w} \right)^2 = 16 \left( \frac{Z_s}{w} \right)^2 \quad \dots \text{eq. 2.2}$$

Where;

$Z_f$  is the distance traveled by the mobile phase front,

$Z_s$  is the distance of traveled by the analyte front, and

$w$  is a spot width of the developed sample spot.

The plate number is dependent on the migration distance and efficiency must be reported in a specific  $R_f$  value of a compound.

## 2.4 Nitrogen adsorption-desorption analysis

Nitrogen adsorption-desorption technique are commonly used for determining the physical properties of the material, such as surface area, pore volume, pore diameter, and pore size distribution. Adsorption of gas by a porous material is described by an adsorption isotherm. The amount of adsorbed gas by the material at constant temperature as a function of pressure. Porous materials are frequently characterized in terms of pore sizes derived from gas sorption data.

### 2.4.1 Classification of adsorption isotherm

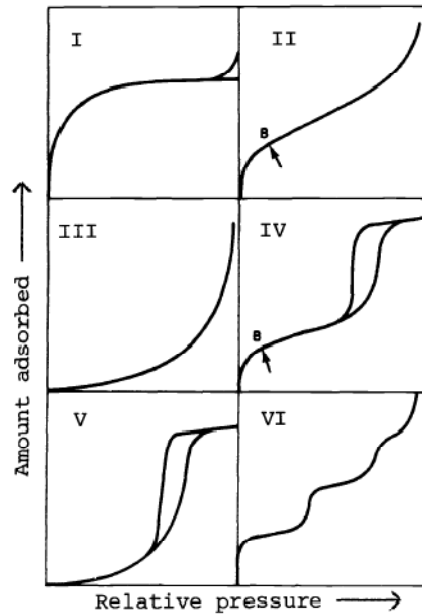


**Figure 2.5** The IUPAC classification of adsorption isotherm [46].

Adsorption isotherm is the relation between the quantity adsorbed and the composition of the bulk phase or the partial pressure in the gas phase under equilibrium conditions at constant temperature.

**Table 2.2** Pore features of adsorption isotherm.

Adsorption type	Pore feature
I	Micropore
II	Nonporous
III	Nonporous
IV	Mesoporous
V	Micropore or Mesoporous
VI	Nonporous

**Table 2.3** IUPAC classification of pores [47].

<b>Pore type</b>	<b>Pore diameter (nm)</b>
Micropore	Up to 2
Mesopore	2 to 50
Macropore	50 to up

According to the IUPAC definition, mesoporous materials exhibit a Type IV adsorption-desorption isotherm as shown in Figure 2.5. At low relative pressure ( $p/p_0$ ), adsorption only occurs as a thin layer on the wall (monolayer coverage). After that, a sharp increase is seen at relative pressure from 0.25 to 0.5, depending on pore size. That corresponds to the capillary condensation of  $N_2$  in the mesoporous. The sharpness of the inflection reflects uniformity of pores and height indicates pore volume.

## **CHAPTER III**

### **EXPERIMENTAL**

#### **3.1 Materials and chemicals**

##### **3.1.1 Preparation of titania nanofibers**

- 1) Polyvinylpyrrolidone, PVP (MW ~1,300,000 g/mol, Sigma Aldrich, Germany)
- 2) Titanium tetraisopropoxide, TTiP 97% (Sigma Aldrich, Germany)
- 3) Absolute ethanol (Merck, Germany)
- 4) Glacial acetic acid (Merck, Germany)

##### **3.1.2 Thin layer chromatography**

- 1) Methyl violet (Riedel-de Haën, Germany)
- 2) Methylene blue hydrate (Fluka, Germany)
- 3) Congo red (Merck, Germany)
- 4) Isopropanol (J.T. Baker, USA)
- 5) 28% Ammonium hydroxide solution (QRęc, New Zealand)
- 6) TLC aluminum sheet with silica 60 F<sub>254</sub> (Merck, Germany)



## 3.2 Methodology

### 3.2.1 Preparation of electrospun fibrous titania

A TTiP sol-gel solution was prepared by the following procedure. Firstly, PVP was dissolved in ethanol. TTiP as the titania precursor was added into the PVP solution and 1.90 mL acetic acid was quickly added into the solution. The solution was placed in an ice-water bath and stirred for 10 min. The amounts of TTiP loading in the polymer solutions examined in this work are summarized in Table 3.1. Later, the obtained solution was transferred into a 5 mL syringe equipped with 21 gauge needle. The electrospinning system was set up in vertical. Electric potential (Matsusada Precision, EQ-30) of 20 and 25 kV was applied to the needle. The solution was pumped by syringe pump (Prosense, NE-1000) at a flow rate of 15, 20 and 25  $\mu\text{L}/\text{min}$ . Aluminum foil and glass slide were used as the collector and placed at 7, 10 and 15 cm below the needle tip. The collected fibers, called as-spun fibers, were heated to 450, 500 and 550°C at a rate of 1°C/min for 3 h using air furnace (Nabertherm, LT 5/11/P330) to obtain the crystallization of the titania fibers, called electrospun fibrous titania.

**Table 3.1** Compositions of polymer solutions and PVP:TiO<sub>2</sub> ratios.

Sample number	Polymer solution		TTiP (g)	Calculated Titania percentage after hydrolysis (By weight, PVP:TiO <sub>2</sub> )
	PVP (g)	Ethanol (mL)		
1	0.42	7	3.00	66.7 (1:2)
2	0.42	7	1.50	50.0 (1:1)
3	0.42	7	0.75	33.3 (2:1)

Aluminum foil and glass slide were used as the collector for comparing the effect of using different collectors. To improve bonding strength between fibers

and collector, spin coating technique was used. The glass slide was set on the sample stage of a spin coater (SCS, G3P-8). The same solution used as the electrospinning precursor solution was spin-coated onto the glass slide at 3,000 rpm for 30 sec (speed to 3,000 rpm within 4 sec). The spin-coated glass was used as the collector for an electrospinning step.

To confirm that the TTiP does not bond with carbonyl groups in the PVP rather than polycondensate, Fourier-transform infrared spectrometry (FT-IR, Nicolet 6700) was used. PVP fibers and the as-spun fibers were characterized with FT-IR by KBr pellet with a range of 4,000-400  $\text{cm}^{-1}$  and 32 scans with resolution of wavenumber of 4  $\text{cm}^{-1}$ .

### **3.2.2 Characterization of electrospun fibrous titania**

#### **3.2.2.1 Morphology of as-spun fibers and electrospun fibrous titania**

The Scanning electron microscope (SEM) photographs were used to determine the morphology, thickness and diameter of the as-spun fibers and the electrospun fibrous titania. They were taken on a JEOL Scanning electron microscope (JSM-5410 LV) at 15 kV and magnification of 10,000. Image Tool 3.0 software (Shareware provided by UTHSCSA) was used for the estimation of diameters of these fiber mats. Thirty different fibers in the image were randomly chosen and measured.

The Transmission electron microscope (TEM) photographs were collected in order to determine the morphology for the electrospun fibrous titania. The TEM photographs were taken on a JEOL Transmission electron microscope (JEM-2100).

### 3.2.2.2 Crystalline structure of electrospun fibrous titania

The structure and crystal size of the electrospun fibrous titania were obtained by X-ray powder diffractometer (XRD, Rigaku Dmax 2200 Ultima Plus) with a monochromator and Cu-K $\alpha$  radiation operated at 40 kV and 20 mA. The XRD patterns were collected in  $2\theta$  range of 10 to 80 degree at a scan rate of 5 degree/min and a scan step of 0.02 degree.

### 3.2.2.3 Nitrogen adsorption-desorption analysis

The nitrogen adsorption-desorption isotherms of the electrospun fibrous titania were measured by a surface area analyzer (BEL, BELSORP Mini). The Brunauer-Emmett-Teller (BET) equation from adsorption-desorption isotherms were calculated for the determination of specific surface area and monolayer volume. The Barrett-Joyner-Halenda (BJH) was calculated to obtain the pore size distribution of the fiber.

### 3.2.3 Thin layer chromatography

Electrospun fibrous titania and conventional particulate silica TLC were tested for separation of dye compounds containing basic group and the efficiency of the TLC separation. The electrospun fibrous titania and particulate silica stationary phases were cut into rectangular plates with the length about 1-2 cm. The fibers were attached on the aluminum plate by adhesive tape and used as stationary phase. They were placed into the mobile phase chamber which was the mixture of ethanol, isopropanol and 2 M ammonium hydroxide (4:4:1 v/v). The developing time of the mobile phase front was observed. A graph between developing time and distance of the mobile phase front was plotted.

The conditions of TLC separations on both TLC plates were summarized in Table 3.2. The test analytes were 0.01 M congo red, 0.005 M methylene blue hydrate and 0.005 M methyl violet. The plates were developed using

4 mL of mobile phase in 50 mL beaker covered with a watch glass. To ensure the air space in the beaker is saturated with mobile phase vapor, a piece of filter paper was placed around and touched the inside wall of the beaker for several minutes. The efficiency of the TLC separation is calculated by eq. 3.1.

$$N = 16 \left( \frac{Z_s}{w} \right)^2 \quad \dots \text{eq. 3.1}$$

Where;

$N$  is the effective plate number,

$Z_s$  is the distance traveled by the analyte front, and

$w$  is the width of the developed sample spot.

The efficiency of TLC relate to a theoretical plate height of the TLC plate as

$$H = \frac{L}{N} \quad \dots \text{eq. 3.2}$$

Where;

$H$  is the effective plate height, and

$L$  is the length of the TLC plate.

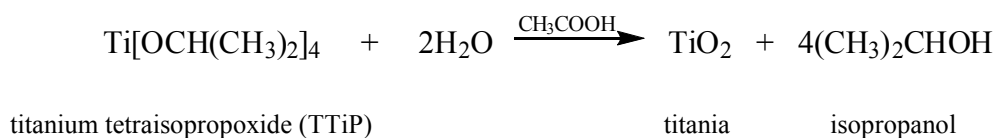
**Table 3.2** Conditions of TLC separations.

	<b>Electrospun fibrous titania TLC</b>	<b>Particulate silica TLC</b>
Developing Distance	1.40-2.00 cm	2.00 cm
Analyte volume	0.10 $\mu$ L	1.00 $\mu$ L
Mobile phase volume	4.00 mL	4.00 mL
Developing time	2 min	5 min

## CHAPTER IV

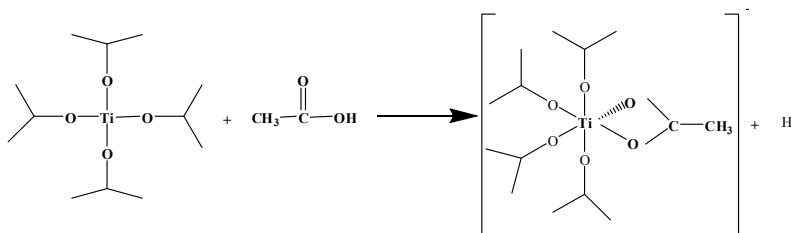
### RESULTS AND DISCUSSION

The titania sol-gel prepared by mixing of polyvinylpyrrolidone (PVP), ethanol (EtOH), titanium tetraisopropoxide (TTiP) and glacial acetic acid was applied for electrospinning process.



**Scheme 4.1** Hydrolysis of TTiP.

The TTiP was hydrolyzed with acetic acid as a catalyst to convert into the titania as in Scheme 4.1. PVP increased the viscosity of the sol-gel solution and prevented the coagulation of titanium precursors; therefore, led to easy fabrication of the fibers. To confirm that the TTiP did not bond with carbonyl of amide group of PVP rather than polycondensate, FT-IR was used to analyze the PVP and the as-spun fibers. The spectra are shown in Fig. 4.1. With observation in both Fig. 4.1 (a) and (b), the broad band at  $3435 \text{ cm}^{-1}$  showed the presence of O–H bond of water which adsorbed on PVP. The peak at  $2953 \text{ cm}^{-1}$  indicated the C–H stretching of the PVP. The peak at  $1655 \text{ cm}^{-1}$  indicated the carbonyl stretching vibration of amide group of the PVP and the peak at  $1545 \text{ cm}^{-1}$  showed the COO vibration of the chelating bidentate structure of intermediate of TTiP and acetic acid as in Scheme 4.2. The FT-IR result suggested that TTiP did not react with the polymer.



**Scheme 4.2** The expected reaction pathway of TTiP and acetic acid.

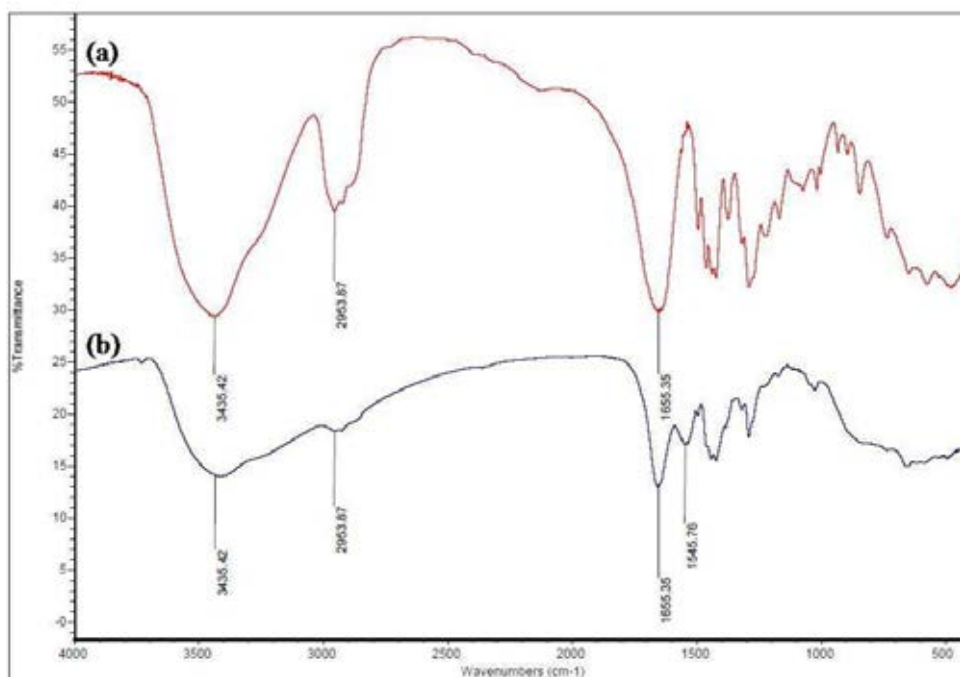


**Figure 4.1** The IR spectra of the fibers of (a) PVP fibers and (b) the as-spun fibers.

#### 4.1 Morphology of electrospun fibrous titania

The morphology of electrospun fibers depended on various parameters of the electrospinning process such as the electric potential, the distance between a needle and a collector, the flow rate of the solution, and the solution concentration. Moreover, the temperature for calcination is one of the factors affecting on the morphology of the fiber.

The solution which was the mixture of PVP, EtOH, TTiP, and glacial acetic acid were fabricated with an electrospinning method. The as-spun fibers were further calcinated to achieve electrospun fibrous titania. SEM images of the as-spun fibers and the electrospun fibrous titania are shown in Fig. 4.2 and Fig. 4.3, respectively. Their average diameters are summarized in Table 4.1.

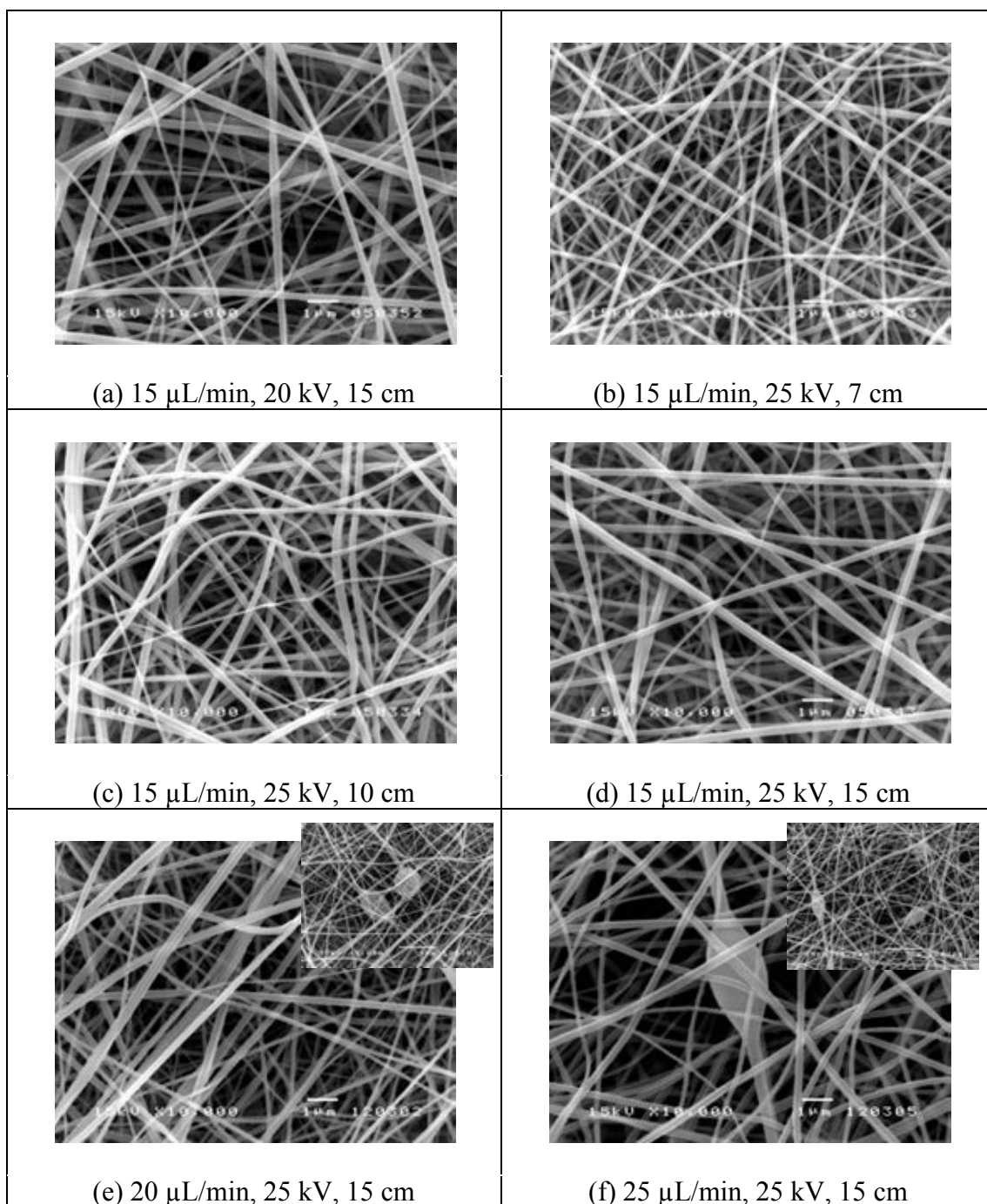


**Figure 4.2** SEM images of the as-spun fibers at various conditions of the flow rate of the solution, the electric potential and the distance between a needle and a collector. The original magnification of 10,000x.

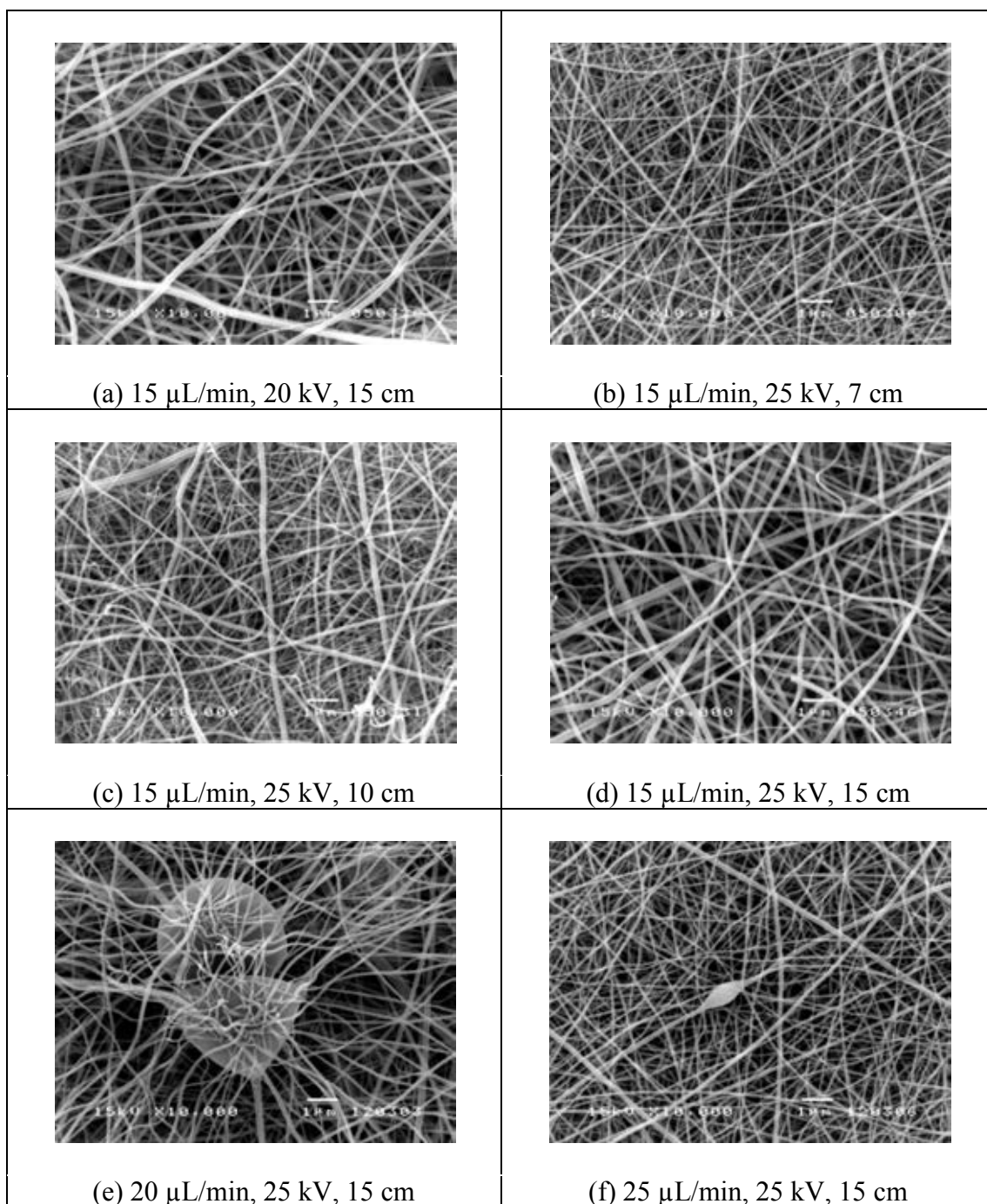


**Figure 4.3** SEM images of the electrospun fibrous titania at various conditions of the flow rate of the solution, the electric potential and the distance between a needle and a collector. The fibers were calcined at 450°C for 3 h. The original magnification of 10,000x.



**Table 4.1** Average diameters of the as-spun fibers and the electrospun fibrous titania at the calcination temperature of 450°C for 3h.

	Flow rate ( $\mu\text{L}/\text{min}$ )	Electric potential (kV)	Distance (cm)	Average diameters of the as-spun fibers (nm, n=30)	Average diameters of the titania fibers (nm, n=30)
(a)	15	20	15	230 $\pm$ 60	140 $\pm$ 30
(b)		25	7	150 $\pm$ 40	80 $\pm$ 30
(c)			10	170 $\pm$ 60	90 $\pm$ 30
(d)			15	210 $\pm$ 40	130 $\pm$ 20
(e)	20	25	15	190 $\pm$ 90	130 $\pm$ 50
(f)	25	25	15	200 $\pm$ 40	110 $\pm$ 30

After calcination, the average diameters of the electrospun fibrous titania of all conditions were smaller than those of the as-spun fibers due to the decomposition of the PVP and consequently the sintering of titania crystallites.

At two different electric potentials (20 and 25 kV), the flow rate of 15  $\mu\text{L}/\text{min}$  and the distance of 15 cm, the as-spun fibers were smooth as in Fig. 4.2 (a) and (d). The average diameter of the as-spun fibers at the electric potential of 20 kV (230 $\pm$ 60 nm) was not significantly different from that of 25 kV (210 $\pm$ 40 nm); nonetheless, an increasing of the electric potential could decrease the size of the as-spun fibers. Increasing the electric potential will increase mass transfer as charged jets of the solution will travel from the needle to the collector at faster rate, resulting in the decreasing of the fiber diameter. Higher electric potential than 25 kV was not suitable for electrospinning because the evaporation of the solvent and acid caused the electric spark. Moreover, the electric potential lower than 20 kV was not enough to fabricate the fiber, leaving some parts of solution at the needle tip.

The characteristics of the as-spun fibers at various distances between a needle and a collector (7, 10 and 15 cm), with the constant flow rate of 15  $\mu\text{L}/\text{min}$  and the electric potential of 25 kV were fine and smooth. The SEM images of the as-spun fibers and the electrospun fibrous titania were shown in (b), (c) and (d) in Fig. 4.2 and

Fig. 4.3, respectively. The average diameters of the as-spun fibers and the electrospun fibrous titania were range of 150-210 and 80-130 nm, respectively. Generally, the gap distance between a needle and a collector affects the time for evaporation of the solvent. As a result, when the gap distance increased, the fiber diameters decreased. However, the result here was inverted such that the diameters increased as increasing the gap distance. The result indicated that the evaporation of solvent was not an important effect. This could be explained that reducing the distance has the similar effect as increasing the electric potential strength per a distance unit (ex. kV/cm). Therefore, reducing the distance led to greater stretching of the solution and decreased the fiber diameters as a consequence.

Most of the as-spun fibers and the electrospun fibrous titania prepared at various flow rates of the solution (15, 20 and 25  $\mu\text{L}/\text{min}$ ), the electric potential of 25 kV and the distance between a needle to a collector of 15 cm were not smooth and uniform. Beads and fiber conjunction were formed as in Fig. 4.2 and 4.3. It caused from the flow rate exceeded a critical value that created unstable jets and consequently formed fibers with large beads. The average fiber diameter obtained at the flow rates of 20 and 25  $\mu\text{L}/\text{min}$  were not significantly different from that obtained at the flow rate of 15  $\mu\text{L}/\text{min}$ . The range of diameter was between 100-200 nm as shown in Table 4.1.

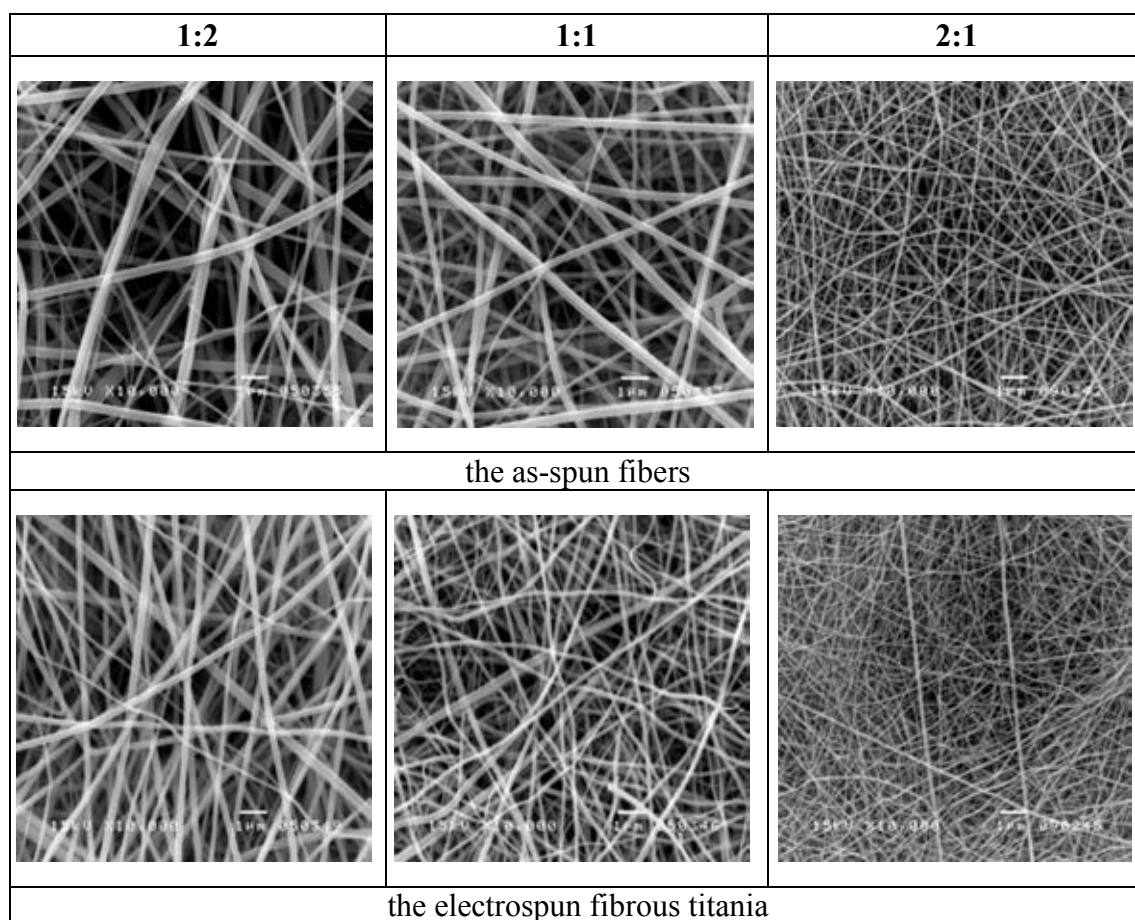


**Figure 4.4** SEM images of the electrospun fibers at various PVP:TiO<sub>2</sub> ratios (by weight). The original magnification of 10,000x (the flow rate of 15  $\mu$ L/min, the electric potential of 25 kV, the distance between a needle and a collector of 15 cm and the calcination temperature of 450°C for 3 h).

**Table 4.2** Average diameters of the as-spun fibers and the electrospun fibrous titania at various PVP:TiO<sub>2</sub> ratios (by weight).

PVP:TiO <sub>2</sub> ratio (by weight)	Average diameters of the as-spun fibers (nm, n=30)	Average diameters of the titania fibers (nm, n=30)
1:2	270 $\pm$ 70	190 $\pm$ 50
1:1	210 $\pm$ 40	130 $\pm$ 20
2:1	90 $\pm$ 20	50 $\pm$ 20

In Fig. 4.4, the SEM images of three samples with different PVP:TiO<sub>2</sub> ratios were shown. The fibers were electrospun at the electric potential of 25 kV, the flow rate of 15  $\mu$ L/min, the distance between a needle and a collector of 15 cm and the calcination temperature of 450°C for 3 h. The obtained fibers from all ratios were smooth and uniform. The average diameter of the electrospun fibrous titania when using the PVP:TTiP ratio of 2:1 was 50 $\pm$ 20 nm. The average diameter of the electrospun fibrous titania at the ratio of 1:1 and 1:2 increased to 130 $\pm$ 20 and 190 $\pm$ 50 nm, respectively. The electrospun fibrous titania when using the ratio of 1:2 had the largest diameter due to the highest concentration of TTiP. Increasing the ratio of TTiP could increase the solution viscosity and led to the larger as-spun fibers. More obviously, when the weight ratio of TTiP increased in as-spun fibers, the calcination product that was comprised mainly of titania, would be larger as well.

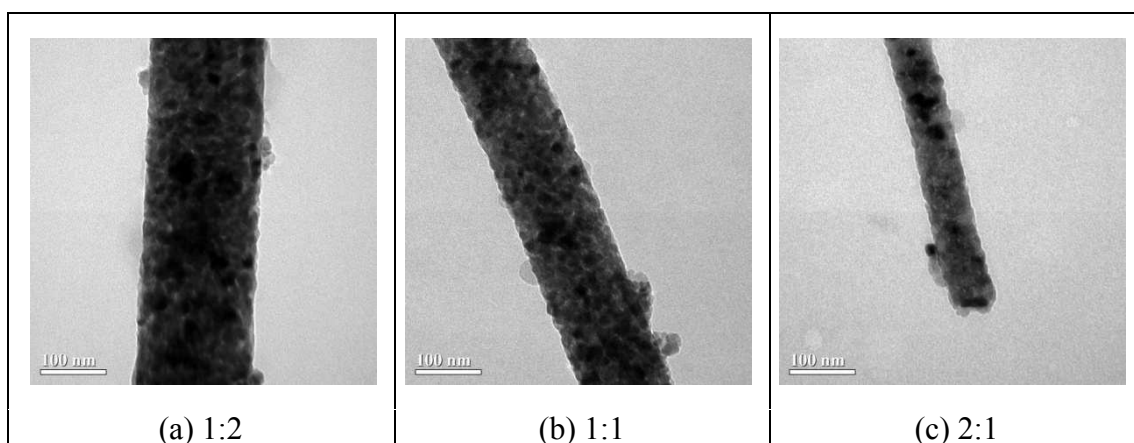


**Figure 4.5** TEM images of the electrospun fibrous titania with PVP:TiO<sub>2</sub> ratios of (a) 1:2, (b) 1:1 and (c) 2:1 by weight.

TEM images of the electrospun fibrous titania at various PVP:TiO<sub>2</sub> ratios were shown in Fig. 4.5. After calcination, PVP was decomposed so the fiber showed only the titania particle. The diameters of the electrospun fibrous titania when using the PVP:TTiP ratio of 1:2, 1:1 and 2:1 were 178, 133 and 67 nm, respectively, which agreed with the SEM observations.

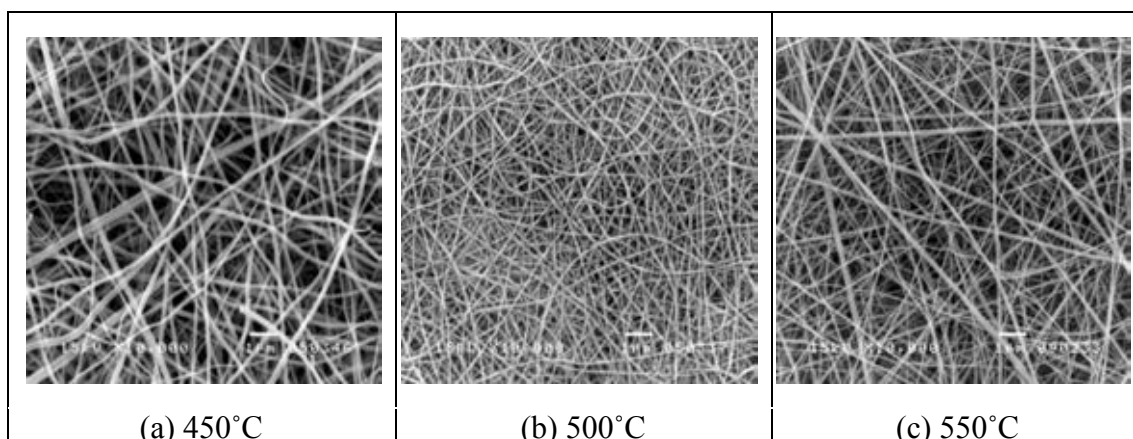


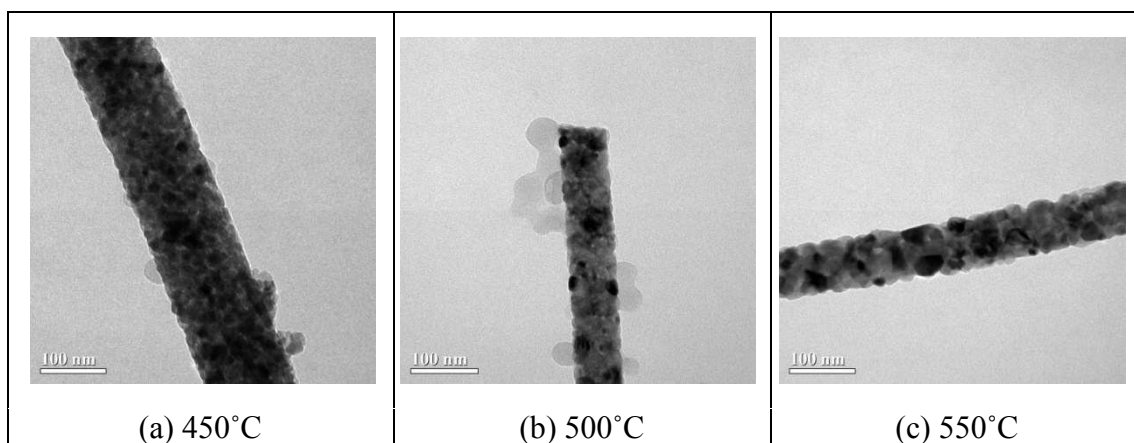
**Figure 4.6** SEM images of the electrospun fibrous titania at various calcination temperatures. The original magnifications of 10,000x (the flow rate of 15  $\mu\text{L}/\text{min}$ , the electric potential of 25 kV, the distance between a needle and a collector of 15 cm and the PVP:TiO<sub>2</sub> ratio of 1:1 by weight).

**Table 4.3** Average diameters of the electrospun fibrous titania at various calcination temperatures for 3 h.

Calcination temperature (°C)	Average diameters of the titania fibers (nm, n=30)
450	130±20
500	70±20
550	80±30

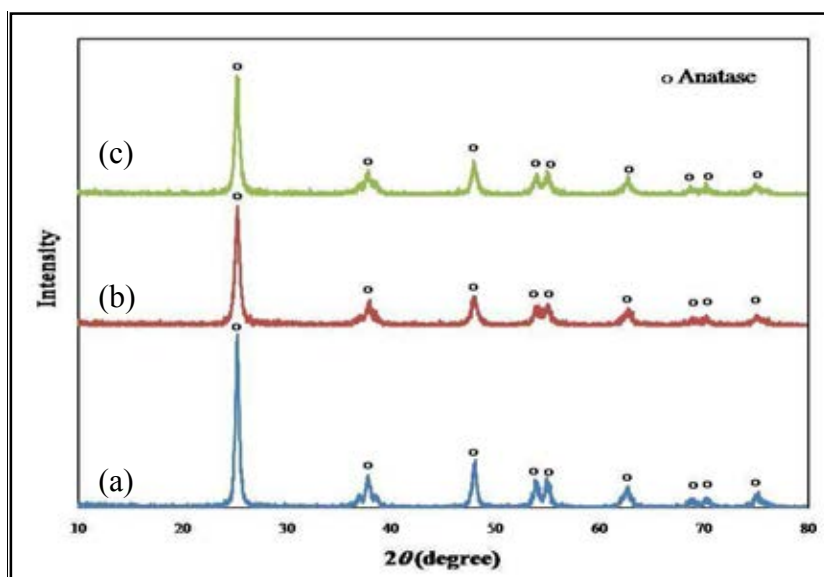
Calcination temperatures were studied at 450, 500 and 550°C for 3 h with the control condition: the electric potential of 25 kV, the flow rate of 15  $\mu\text{L}/\text{min}$ , the distance between a needle and a collector of 15 cm and the PVP:TiO<sub>2</sub> ratio of 1:1 by weight. Fig. 4.6 showed the SEM images of the electrospun fibrous titania at different temperatures. The electrospun fibrous titania had uniform diameters. When the temperature increased, the average diameter decreased (Table 4.3). This could be explained as the shrinkage of the electrospun fibrous titania due to the sintering of titania particles. At high temperatures, the atoms of small titania particles could diffuse and fuse with each others to become larger particles as the TEM images in

Fig. 4.7. The driving force of the sintering process is to reduce the surface energy and lead to the shrinkage of the workpieces.



**Figure 4.7** TEM images of electrospun fibrous titania with calcination temperatures of (a) 450°C, (b) 500°C and (c) 550°C for 3 h.

## 4.2 Crystalline structure of electrospun fibrous titania



**Figure 4.8** XRD patterns of the electrospun fibrous titania with PVP:TiO<sub>2</sub> ratios of (a) 1:2, (b) 1:1 and (c) 2:1 by weight.

The electrospun fibrous titania from electrospinning at the PVP:TiO<sub>2</sub> ratios of 1:1, 1:2 and 2:1 by weight were calcinated at 450°C for 3 h. The crystalline structure of the fibers was characterized by X-ray diffraction. Diffraction peaks as shown in Fig. 4.8 correspond to an anatase phase according to 21-1272.

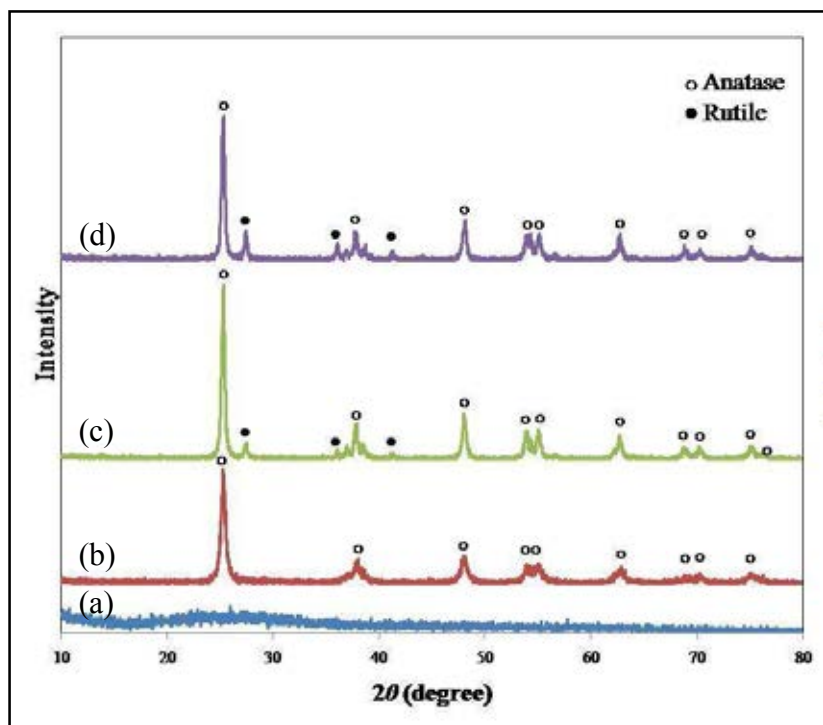


**Figure 4.9** XRD patterns of (a) the as-spun fibers and the electrospun fibrous titania after calcination at (b) 450°C, (c) 500°C and (d) 550°C for 3 h.

According to Fig. 4.9, after calcination at 450, 500 and 550°C, the crystallization of titania occurred as the peaks get sharper at higher temperature. However, a rutile phase started to form as the temperature reached 500°C and more at higher temperature. It is well-known that anatase phase is a stable phase of crystalline titania at lower temperature, and rutile phase is the more stable phase at higher temperature [48-50]. Therefore, the products transformed from amorphous to the pure anatase and mixed phase of anatase and rutile as labeled in XRD patterns. The XRD pattern of the as-spun fibers (Fig. 4.9 (a)) showed more amorphous than the electrospun fibrous titania (Fig. 4.9 (b), (c) and (d)). The electrospun fibrous titania

which were calcinated at 450°C for 3 h showed a characteristic of pure anatase crystalline phase (Fig. 4.9 (b)). At higher calcination temperature than 450°C, the XRD pattern showed characteristic of mixed anatase and rutile crystalline phase. With increasing calcination temperature, the intensity of rutile crystalline phase was increased as in Fig. 4.9 (c) and (d).

### 4.3 Nitrogen adsorption-desorption analysis

All the nitrogen adsorption-desorption isotherms of the electrospun fibrous titania showed a type IV of porous materials following the IUPAC (International Union of Pure and Applied Chemistry) that is a characteristics of mesoporous. The type IV isotherm is presented to multilayer adsorption that related to Brunauer-Emmett-Teller (BET) method for calculation of specific surface area and Barrett-Joyner-Halenda (BJH) theory for examined pore size on the electrospun fibrous titania and pore size distribution.

Monolayer volume which is the first layer that the adsorbed gas adsorbs on the material can be calculated by eq. 4.1 and specific surface area which is the total surface area per unit mass can be calculated by eq. 4.2.

$$\frac{p}{V \cdot (p^0 - p)} = \frac{1}{V_m \cdot C} + \frac{(C-1)}{V_m \cdot C} \cdot \frac{p}{p^0} \quad \dots \text{eq. 4.1}$$

Where;

$V$  is the amount of N<sub>2</sub> adsorbed at the relative pressure  $p/p^0$ ,

$V_m$  is the the monolayer adsorbed gas quantity,

$p$  and  $p^0$  are the equilibrium and the saturation pressure of adsorbates, and

$C$  is the BET constant.



$$S_{BET} = \frac{S_{total}}{a} = \frac{V_m \cdot N \cdot s}{M \cdot a} \quad \dots \text{eq. 4.2}$$

Where;

$S_{BET}$  is a specific surface area,

$S_{total}$  is a total surface area,

$a$  is weight of sample solid,

$N$  is Avogadro's number,

$s$  is the average molecular cross-section area, and

$M$  is molecular weight of adsorbate.

In Fig. 4.10, the nitrogen adsorption-desorption isotherms were fitted to BET-Plot as shown in Fig. 4.11. The specific surface area and the monolayer volume which were calculated by the BET equation and the average diameter of pore on the electrospun fibrous titania which were determined by the BJH method were summarized in Table 4.4.

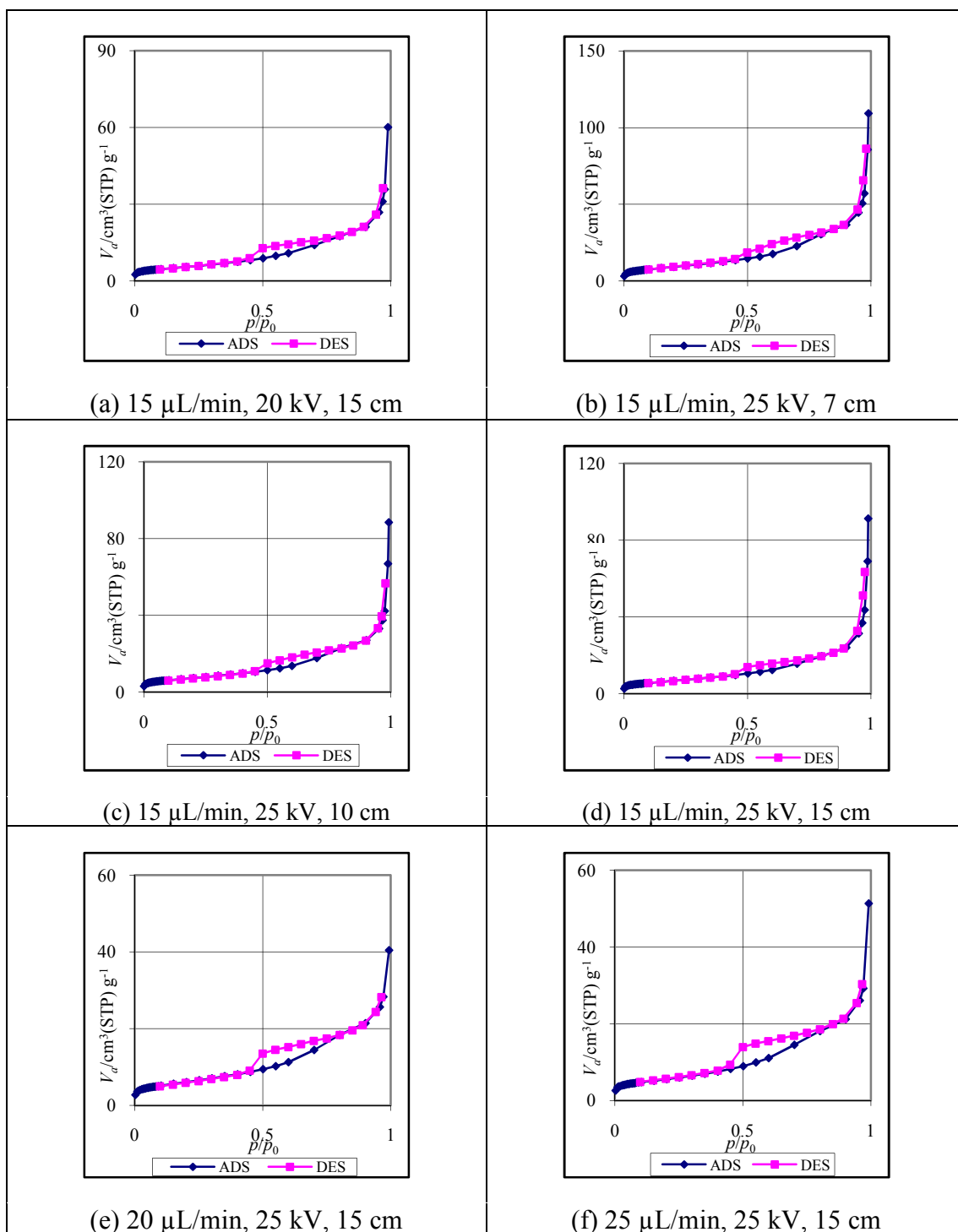


**Figure 4.10** Nitrogen adsorption-desorption isotherms of the electrospun fibrous titania at various conditions of the flow rate of the solution, the electric potential and the distance between a needle and a collector. The fibers were calcined at 450°C for 3 h.

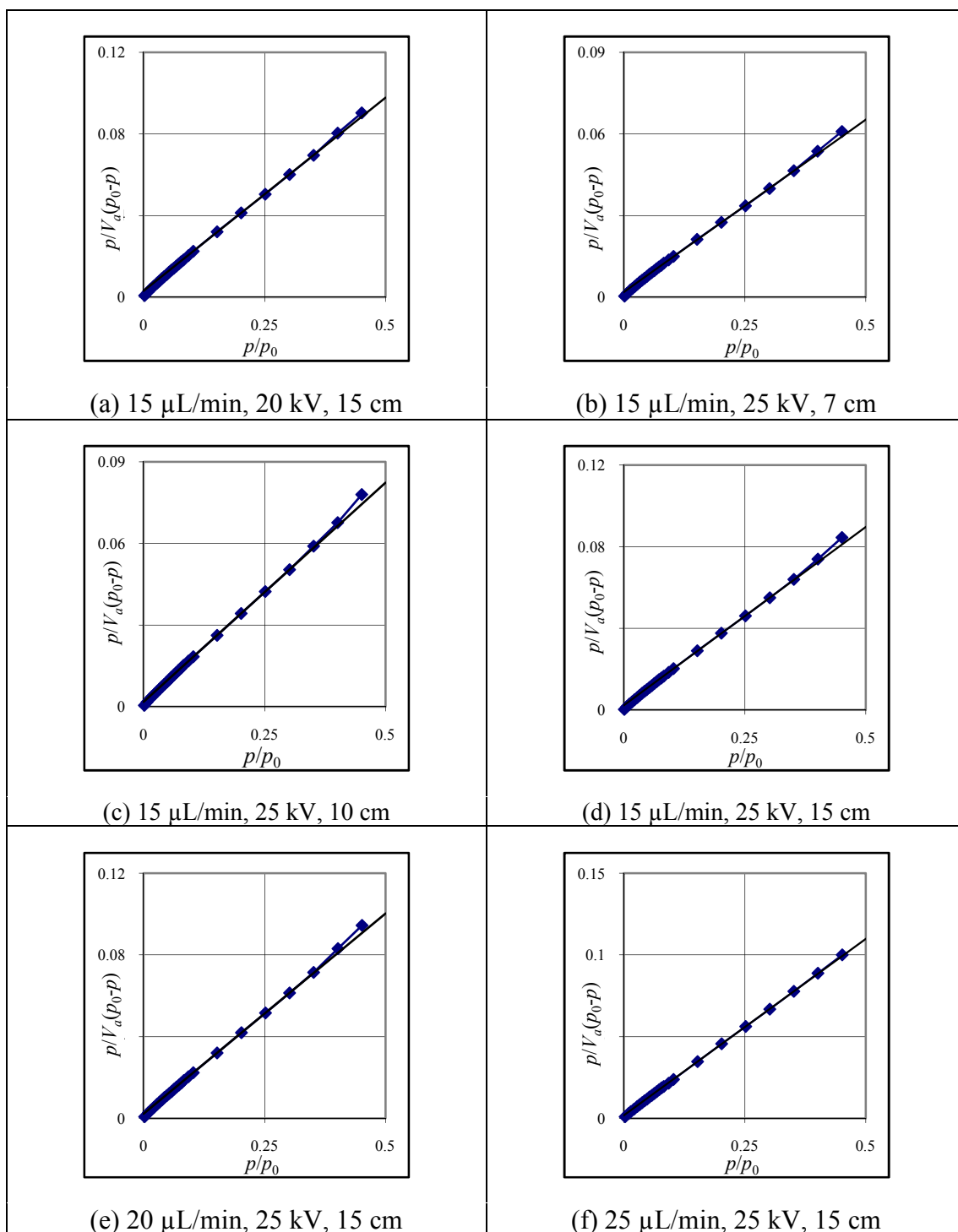


**Figure 4.11** BET-Plots of the electrospun fibrous titania at various conditions of the flow rate of the solution, the electric potential and the distance between a needle and a collector. The fibers were calcined at 450°C for 3 h.

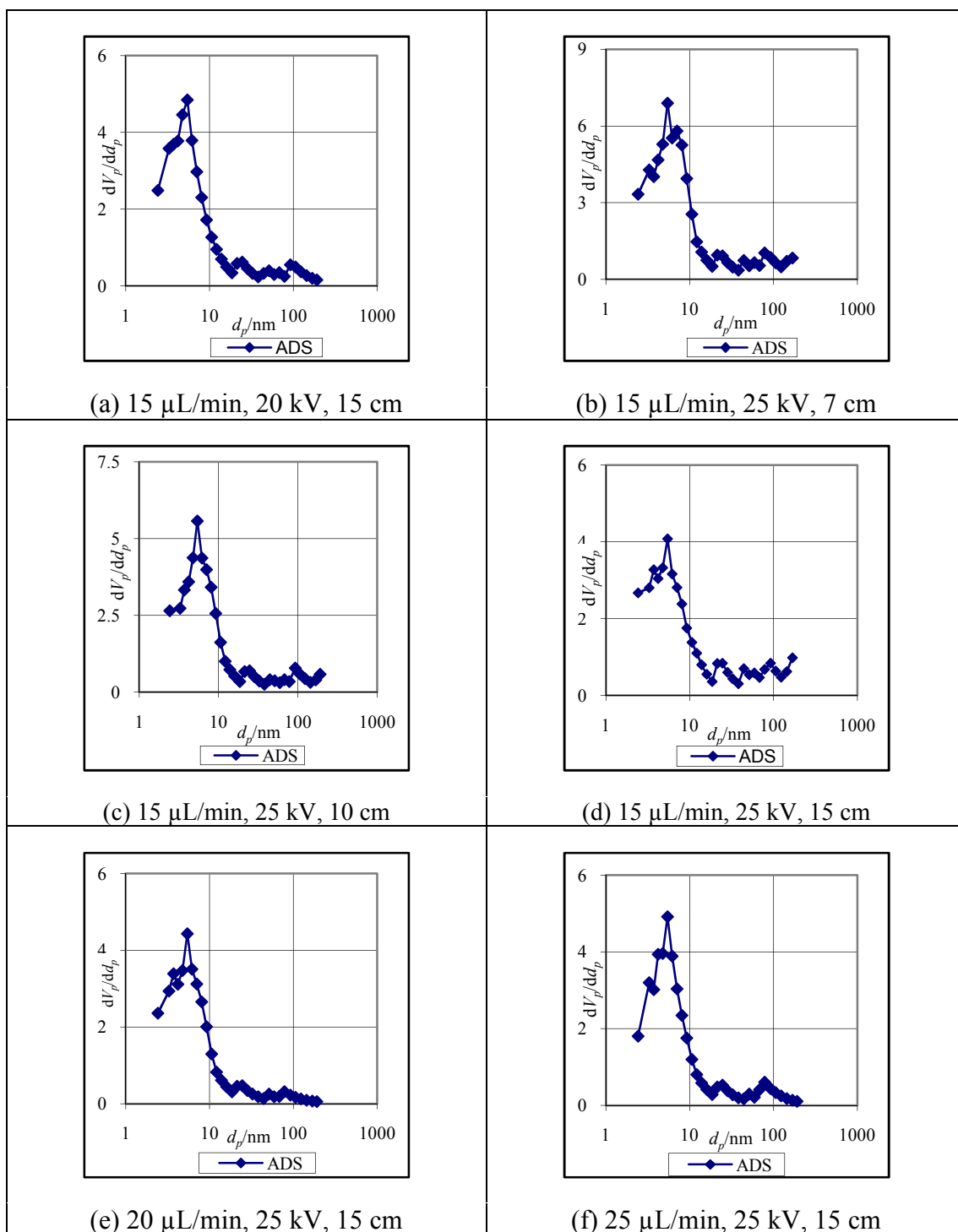


**Figure 4.12** Pore size distribution of the electrospun fibrous titania at various conditions of the flow rate of the solution, the electric potential and the distance between a needle and a collector. The fibers were calcined at 450°C for 3 h.

**Table 4.4** Specific surface area, monolayer volume and average pore diameter of the electrospun fibrous titania at various conditions.

	Flow rate ( $\mu\text{L}/\text{min}$ )	Electric potential (kV)	Distance (cm)	Specific surface area, $S_{BET}$ ( $\text{m}^2 \cdot \text{g}^{-1}$ )	Monolayer volume, $V_m$ ( $\text{cm}^3(\text{STP})\text{g}^{-1}$ )	Average pore diameter, $d_p$ (nm)
(a)	15	20	15	22.625	5.1982	5.41
(b)		25	7	33.820	7.7704	5.41
(c)			10	26.727	6.1407	5.41
(d)			15	24.580	5.6473	5.41
(e)	20	25	15	21.926	5.0376	5.41
(f)	25	25	15	19.967	4.5876	5.41

From Table 4.4 (a) and (d), increasing the electric potential across a needle and a collector, the specific surface area and the monolayer volume increased. These results agree with the SEM images in Fig. 4.3 that show the lower average diameters of the fiber as the electric potential increased. Therefore, the smaller diameters of the fiber offered larger surface area of titania per unit weight. When increasing the distance between a needle and a collector, the average diameter increased that affected on the specific surface area and the monolayer volume. The smallest fiber diameter, distance of 7 cm, had the highest specific surface area and the monolayer volume as in Table 4.4 (b), (c) and (d).

Because of the bead formation and the fiber conjunction, the fibers at the flow rate of 20 and 25  $\mu\text{L}/\text{min}$  (Table 4.4 (e) and (f)) had the specific surface area and the monolayer volume less than the fibers at the flow rate of 15  $\mu\text{L}/\text{min}$  (Table 4.4 (d)). The result matched with the SEM images.

Pore size distribution of the electrospun fibrous titania at various electrospinning conditions was shown in Fig. 4.12. When the electrospinning parameter was changed, the average pore diameter remained constant. These results indicated that the electrospinning condition had no affect on the pore size between the titania particles.

Another parameter which affect the surface characteristics is the PVP:TiO<sub>2</sub> ratio and the calcination temperature. The surface characteristics of the electrospun fibrous titania at different ratio and calcination temperature were shown in Fig. 4.13 and Fig. 4.14, respectively.

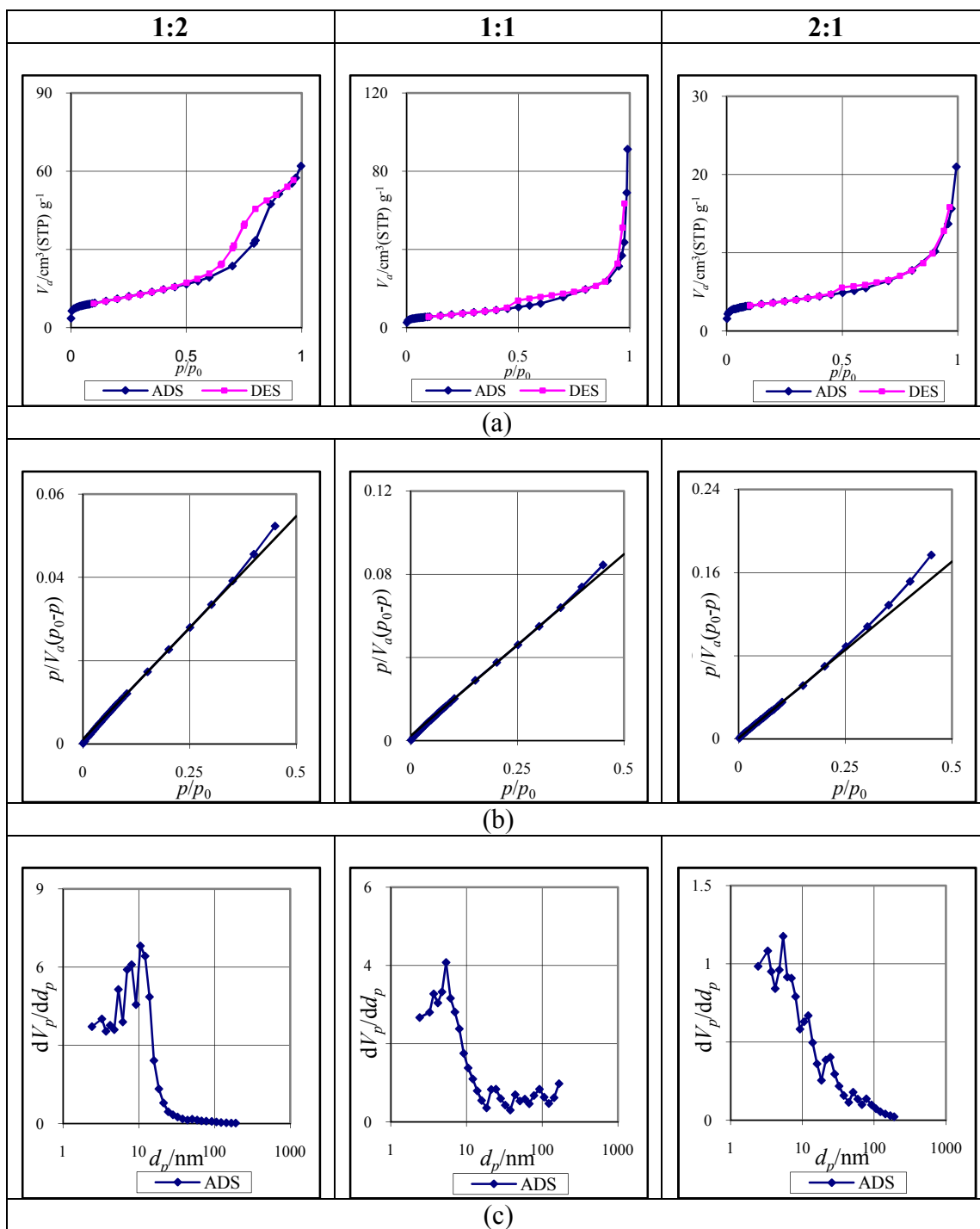


**Figure 4.13** Characteristics of the electrospun fibrous titania at various PVP:TiO<sub>2</sub> ratios: (a) nitrogen adsorption-desorption isotherms, (b) BET-Plots and (c) pore size distributions.

**Table 4.5** Specific surface area, monolayer volume and average pore diameter of the electrospun fibrous titania at various PVP:TiO<sub>2</sub> ratios.

<b>PVP: TiO<sub>2</sub> ratio (by weight)</b>	<b>BET specific surface area, <math>S_{BET}</math> (m<sup>2</sup>·g<sup>-1</sup>)</b>	<b>Monolayer volume, <math>V_m</math> (cm<sup>3</sup>(STP)g<sup>-1</sup>)</b>	<b>Average pore diameter, <math>d_p</math> (nm)</b>
1:2	40.171	9.2294	10.57
1:1	24.58	5.6473	5.41
2:1	12.797	2.9401	5.41

The surface characteristics of the electrospun fibrous titania at various PVP:TiO<sub>2</sub> ratios were shown in Fig. 4.13, and the specific surface area, monolayer volume and pore diameter were calculated by the BET equation and the BJH method as listed in Table 4.5.

The PVP:TiO<sub>2</sub> ratio of 1:2 had the highest specific surface area, monolayer volume and average pore diameter. The lower specific surface area and monolayer volume was observed when PVP:TiO<sub>2</sub> ratio was 1:1 and 2:1. While the average pore diameter of the PVP:TiO<sub>2</sub> ratio of 1:1 and 2:1 were similar but less than that of 1:2. These may cause from the sintering of crystalline titania. As PVP content in the fibers from the PVP:TiO<sub>2</sub> ratio of 1:2 was lower than that of 1:1 and 2:1 (or higher titania content), the sintering of titania crystallites was minimal leading to high specific surface area and monolayer volume of the fibers.



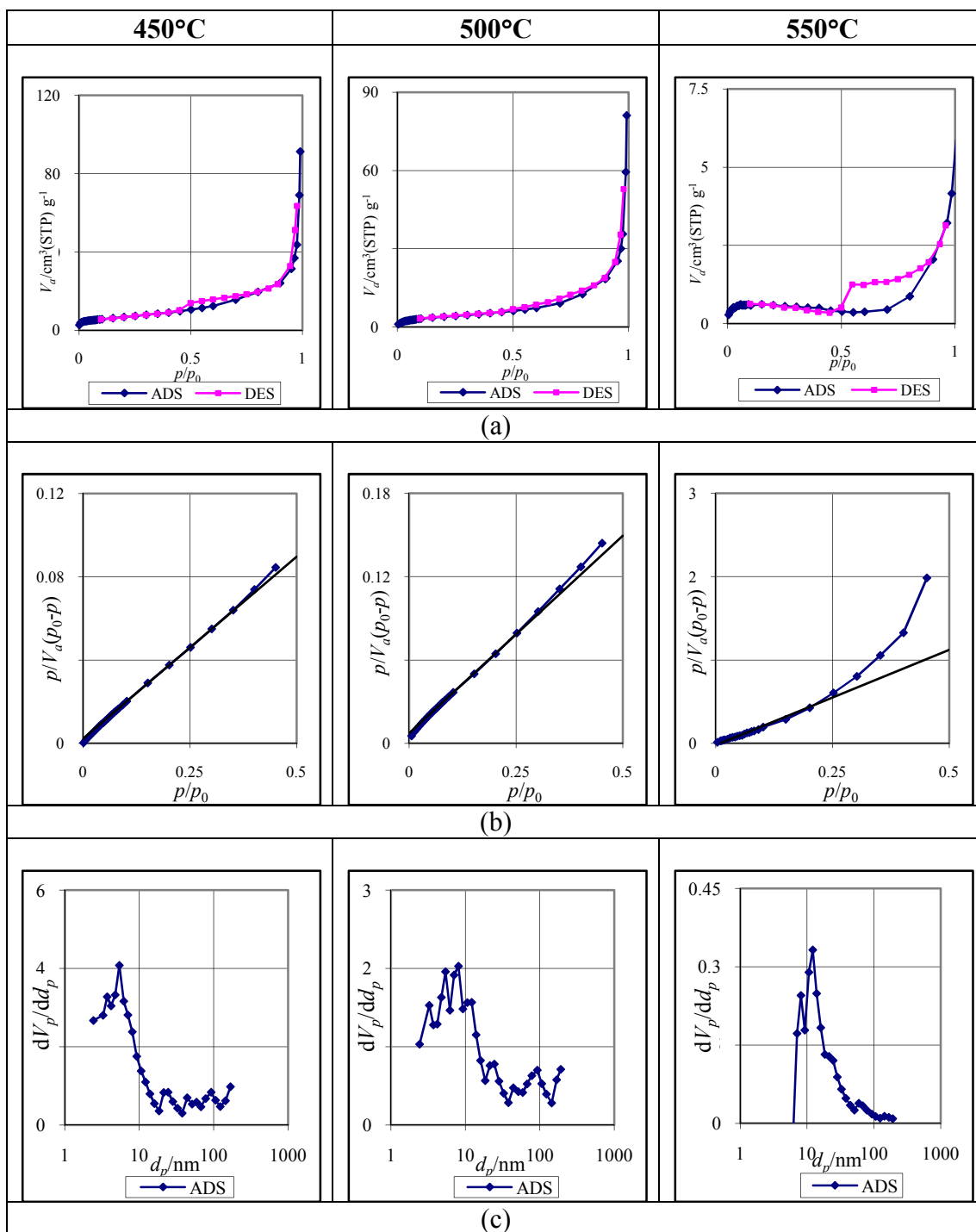


**Figure 4.14** Characteristics of the electrospun fibrous titania at various calcination temperatures: (a) nitrogen adsorption-desorption isotherms, (b) BET-Plots and (c) pore size distributions.

**Table 4.6** Specific surface area, monolayer volume and average pore diameter of the electrospun fibrous titania at various calcination temperatures.

Calcination temperature (°C)	BET specific surface area, $S_{BET}$ ( $\text{m}^2 \cdot \text{g}^{-1}$ )	Monolayer volume, $V_m$ ( $\text{cm}^3(\text{STP})\text{g}^{-1}$ )	Average pore diameter, $d_p$ (nm)
450	24.58	5.6473	5.41
500	14.916	3.4269	8.06
550	1.9197	0.4411	12.12

The specific surface area, monolayer volume and average pore diameter were calculated and listed in Table 4.6. When the calcination temperature increased, the specific surface area and the monolayer volume decreased, but the average pore diameter increased. The decreases of the specific surface area and the monolayer volume were caused by the sintering of the crystalline titania at higher temperature. In addition, the larger pore diameter at higher calcination temperature was due to the higher degree of PVP and organic residues decomposition. Moreover, the transformation of the crystalline titania from pure anatase phase to the mixture of anatase and rutile phases at calcination temperature of 500 and 550°C decreased the surface area [50].

#### 4.4 Effect of the collectors

Various collectors such as aluminum foil, glass slide and spin-coated glass slide were studied. The aluminum foil was wrapped on the copper plate which is the conducting material. The glass slides were used without further cleaning and plated on the copper plate. Before calcination, the as-spun fibers adhered smoothly on both collectors due to the polymer still remained in the as-spun fibers. But after calcination, losing of the polymer and the high calcination temperature caused the shrinkage of the electrospun fibrous titania, resulting to the detachment of the fiber from the collector.

The spin-coated glass slides were the glass slides which were spin-coated with the same electrospinning solution. Then, they were placed on the copper plate as the collector. The result was similar as the aluminum foil and the glass slide that the detachment of the electrospun fibrous titania from the collector was found, but the spin-coated layer still adhered on the glass slide (Fig. 4.15). Thus, there is no chemical bonding between the spin-coated layer and the fibers.

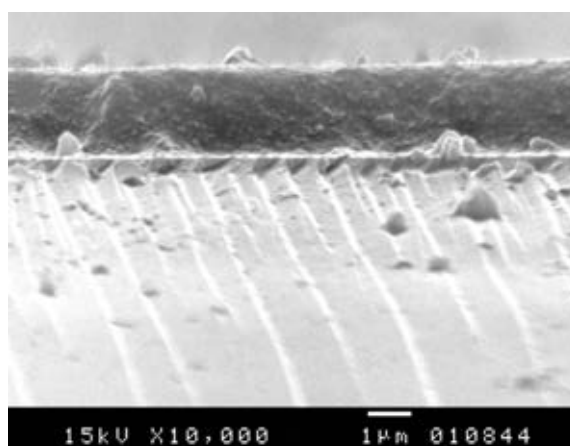


**Figure 4.15** SEM image of the cross section of spin-coated layer.

## 4.5 Thin layer chromatography

From the morphology and characterization of the electrospun fibrous titania described in Section 4.1-4.4, the fibers from five conditions in Table 4.7 were further studied as the stationary phase in thin layer chromatography (TLC). All conditions were electrospun at the solution flow rate of 15  $\mu\text{L}/\text{min}$ , the electric potential of 25 kV, and the distance between a needle and a collector of 15 cm. The thickness about 60  $\mu\text{m}$  which examined from SEM image (Fig. 4.15) was prepared as a stationary phase for TLC separation.

**Table 4.7** Electrospinning conditions for preparation of the electrospun fibrous titania stationary phase.

Stationary phase	PVP:TiO <sub>2</sub> ratio (by weight)	Calcination temperature (°C)
Ti-1:2-450	1:2	450
Ti-1:1-450	1:1	
Ti-2:1-450	2:1	
Ti-1:1-500	1:1	500
Ti-1:1-550	1:1	550

Electrospun fibrous titania from condition Ti-1:2-450, Ti-1:1-450 and Ti-2:1-450 were different in the specific surface area caused by different PVP:TiO<sub>2</sub> ratio at 450°C of calcination where the same crystalline titania phase (anatase phase) was achieved as described previously in Section 4.3.

Electrospun fibrous titania from condition Ti-1:1-450, Ti-1:1-500 and Ti-1:1-550 were different in the specific surface area and the crystalline titania phase as calcination temperature was varied in which PVP:TiO<sub>2</sub> ratio was constant at 1:1 as described previously in Section 4.3.

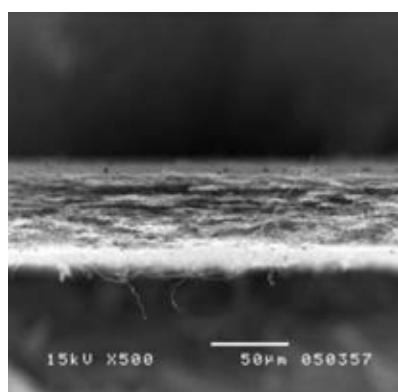


**Figure 4.16** SEM image of the cross section of electrospun fibrous titania at the flow rate of 15 µL/min, the electric potential of 25 kV, the distance between a needle and a collector of 15 cm, the PVP:TiO<sub>2</sub> ratio of 1:1 by weight, the calcination temperature of 450°C and the electrospinning time of 1 h.

#### 4.5.1 Mobile phase transport

The relationship between the distance traveled by the mobile phase front and developing time in TLC can be described by the Lucas-Washburn equation (eq. 4.3).

$$Z_f^2 = \frac{\gamma R t \cos \theta}{2\eta} \quad \dots \text{eq. 4.3}$$

Where;

$Z_f$  is the distance traveled by the mobile phase front,

$\gamma$  is the surface tension of the mobile phase,

$\eta$  is the viscosity of the mobile phase,

$R$  is the equivalent capillary radius,

$t$  is the developing time, and

$\theta$  is the contact angle between the mobile phase and the layer.

And,

$$R = K_0 d_p \quad \dots \text{eq. 4.4}$$

Where;

$K_0$  is the permeability constant of the layer, and

$d_p$  is the average particle size.

The plot of distance traveled by the mobile phase front versus square root of developing time on particulate silica and electrospun fibrous titania TLC (Ti-1:1-450) were shown in Fig. 4.17. The linear fitted with the Lucas-Washburn equation indicated that the mobile phase transport in the electrospun fibrous titania TLC was a capillary flow through porous media similar to that in the particulate silica TLC.

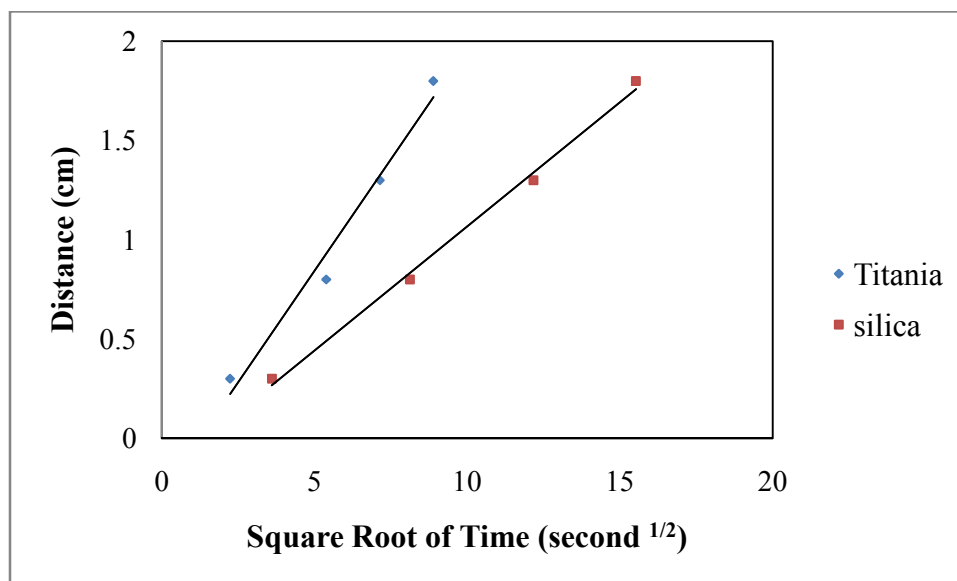


**Figure 4.17** Mobile phase migration distances versus developing time on particulate silica and electrospun fibrous titania TLC plates.

Further understanding the mobile phase transport in the electrospun fibrous TLC, the velocity constant,  $\kappa$ , which used to describe the mobile phase transport in TLC was calculated by eq. 4.5.

$$\kappa = \frac{\gamma R}{2\eta} \quad \dots \text{eq. 4.5}$$

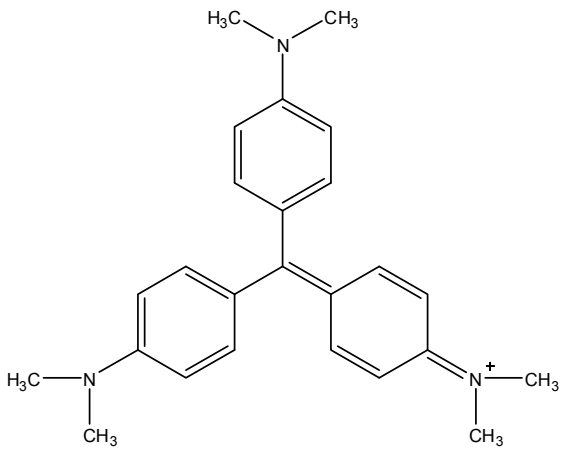
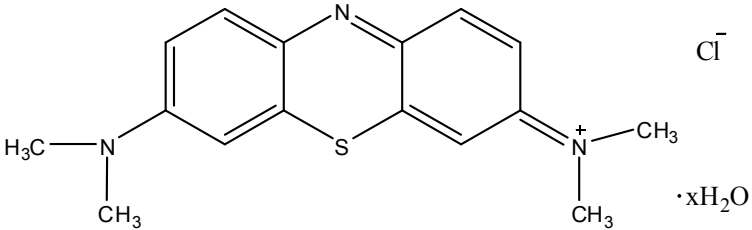
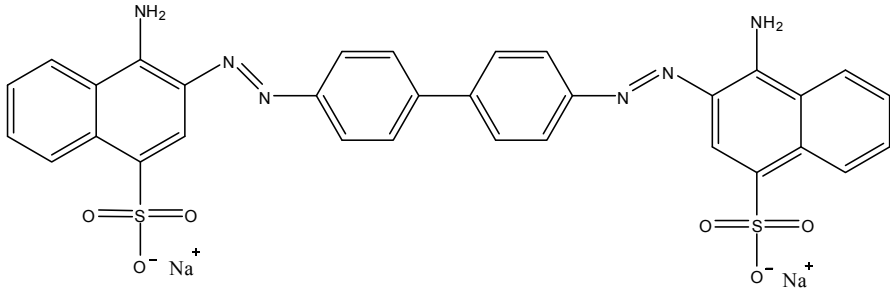
From Table 4.8, the velocity constant of the electrospun fibrous TLC was higher than that of the particulate silica TLC. The faster mobile phase velocities can refer to the larger equivalent capillary radius or the pore radius in stationary phase.

**Table 4.8** Comparison of  $\kappa$  values.

TLC	$\kappa$ (cm <sup>2</sup> /s)
Electrospun fibrous titania	0.050
Particulate silica	0.016

#### 4.5.2 Separation of dyes

The separation of basic compounds was performed to study the chromatographic behavior of the electrospun fibrous titania TLC comparing to the particulate silica TLC. The dye analytes containing basic groups which are methyl violet, methylene blue hydrate and congo red (Fig. 4.18) were selected for this study.

	methyl violet
	methylene blue hydrate
	congo red

**Figure 4.18** The molecular structure of methyl violet, methylene blue hydrate and congo red.

The migration of dye compounds on the electrospun fibrous titania and the particulate silica TLC plates were shown in Fig. 4.19. The average spot width, retardation factor ( $R_f$ ) and plate height of the electrospun fibrous titania and the particulate silica TLC were summarized in Table 4.9.

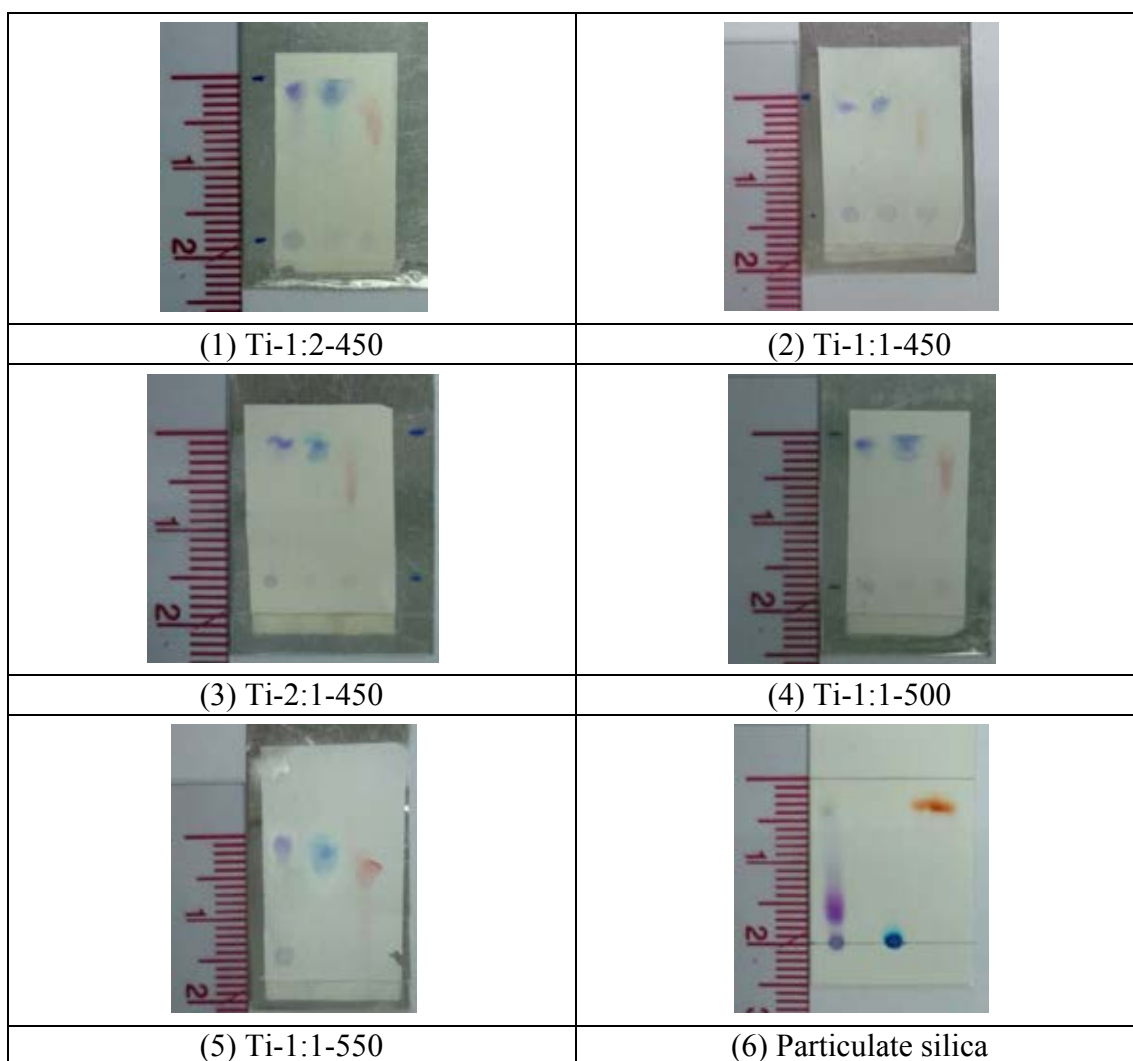


**Figure 4.19** The separation of dye compounds on (1-5) the electrospun fibrous titania TLC from various conditions as shown in Table 4.7 and (6) the particulate silica TLC.



**Table 4.9** Spot width, retardation factor ( $R_f$ ) and plate height ( $H$ ) of dye compounds ( $n=2$ ) for various conditions of the electrospun fibrous titania and the particulate silica TLC.

Stationary phase	Methyl violet			Methylene blue hydrate			Congo red		
	Spot width (cm)	$R_f$	$H$ ( $\mu\text{m}$ )	Spot width (cm)	$R_f$	$H$ ( $\mu\text{m}$ )	Spot width (cm)	$R_f$	$H$ ( $\mu\text{m}$ )
Ti-1:2-450	0.23	0.91	21.86	0.45	0.89	88.99	0.55	0.69	217.8
Ti-1:1-450	0.15	0.93	12.15	0.25	0.96	31.20	0.43	0.67	192.6
Ti-2:1-450	0.23	0.94	24.37	0.35	0.87	65.11	0.45	0.67	177.9
Ti-1:1-500	0.30	0.94	37.35	0.33	0.91	48.16	0.55	0.70	223.2
Ti-1:1-550	0.35	0.87	67.95	0.25	0.90	32.15	0.50	0.63	259.7
Silica	0.75	0.20	4,394	0.28	–	–	0.20	0.85	17.30

The efficiency of TLC can present by the effective plate height which described by van Deemter equation as eq. 4.6.

$$H = A + \frac{B}{u} + Cu \quad \dots\text{eq. 4.6}$$

Where;

$A$  is the contribution to zone broadening by eddy diffusion,

$B$  is the contribution of longitudinal diffusion,

$C$  is the contribution of resistance to mass transfer in both the stationary phase and mobile phase, and

$u$  is the average linear mobile phase velocity.

Comparing the migration of analytes on Ti-1:2-450, Ti-1:1-450 and Ti-2:1-450, the retardation factors for each analyte on different electrospun fibrous titania TLC were similar while the spot bandwidths of all analytes on Ti-1:1-450 were narrower than those on Ti-1:2-450 and Ti-2:1-450. The similarity of retardation factor

would result from the same interaction of analyte and stationary phase because the crystalline titania phases in Ti-1:2-450, Ti-1:1-450 and Ti-2:1-450 were the same which is the anatase phase. The different in spot bandwidth would affect from the pore size distribution of the electrospun fibrous titania TLC where Ti-1:1-450 result the most uniform (Fig. 4.13). The uniformity of the electrospun produced the less different of the analyte zone migrates through the stationary phase that affect on the  $A$ -term in van Deemter equation. If the uniformity of the stationary phase was increased,  $A$ -term will decrease resulting in decreasing of  $H$ . As a result, narrower bandwidth was observed.

Comparing the migration of analytes on Ti-1:1-450, Ti-1:1-500 and Ti-1:1-550, the retardation factor on different electrospun fibrous titania TLC were similar while the spot bandwidths of all analytes on Ti-1:1-450 were narrower than those on Ti-1:1-500 and Ti-1:1-550. These would result from the pore size distribution of the fibers (Fig. 4.14) which were similar with the effect of the PVP:TiO<sub>2</sub> ratio. Moreover, the plate height of these electrospun fibrous titania TLC plates were agreed with the pore size distribution. Although, phase transformation of the titania was showed at higher calcination temperature, the major phase was anatase so the phase properties was less affecting on the TLC efficiency. And the results showed the uniformity of the pore size distribution was more effective on the TLC efficiency than the phase properties.

The separation results of both electrospun fibrous titania and particulate silica TLC were different. Methyl violet and methylene blue hydrate was able to travel on the electrospun fibrous titania TLC while they were retained on the particulate silica TLC. On the other hand, congo red traveled on the particulate silica TLC better than that on the electrospun fibrous titania TLC. The results caused by the different polarity of the titania and silica as stationary phase. Under basic condition of TLC development, silanol group of the silica is more acidic [8, 27-28] than the titania [8, 27-30] resulting in the negatively charge of the silica and slightly positive of the titania. While the methyl violet and the methylene blue hydrate were protonated at the amine group resulting in positively charge so they interact strongly with the silica surface. But congo red was deprotonated at sulfonate groups resulting in negatively

charged so congo red can travel on particulate silica TLC better than methyl violet and methylene blue hydrate. On the other hand, the electrospun fibrous titania TLC is slightly basic at this condition. Therefore, all analysts can travel on the electrospun fibrous titania TLC.

## CHAPTER V

### CONCLUSION

#### 5.1 Conclusion

From the preparation of the electrospun fibrous titania via sol-gel process and fabrication with electrospinning method, the fibers had been successfully generated with the smooth and uniform morphology with the diameters range of 50-190 nm. The as-spun fibers were characterized by Fourier-transform infrared spectrometer (FT-IR) and indicated that TTiP did not bond with carbonyl groups in the PVP. The morphology of the as-spun fibers and the electrospun fibrous titania were characterized by scanning electron microscope (SEM), transmission electron microscope (TEM), X-ray powder diffractometer (XRD), and surface area analyzer. The morphology and the diameter of the fibers were affected by the electric potential, the distance between a needle and a collector, the flow rate of the solution, the ratio of PVP:TiO<sub>2</sub> and the calcination temperature. Increasing the electric potential, the fiber diameter decreased while the flow rate of the solution and the distance between a needle and a collector increased, the size of the fiber increased. Higher PVP:TiO<sub>2</sub> ratio led to the smaller fiber diameter, specific surface area and pore size of the titania. At higher calcination temperature, the specific surface area of the fibers decreased and the pore size increased. In addition, the electrospun fibrous titania was crystallized and formed the anatase phase at calcinations temperature of 450°C. Moreover, partially change from anatase to rutile phase was observed when calcination temperature was increased to 500 and 550°C.

In thin layer chromatography, the electrospun fibrous titania can be used as the stationary phase. The mobile phase velocity in electrospun fibrous titania TLC was faster than that in conventional silica TLC. Moreover, the efficiency of dye separation using the electrospun fibrous titania TLC was better than the silica TLC.

The electrospun fibrous titania were successfully prepared by electrospinning method for using as new alternative stationary phase in thin layer chromatography. It can be used for the separation of basic compounds.

## **5.2 Suggestion of future work**

In this experiment, the major phase of the titania was anatase. Since some properties of the anatase phase are different from the rutile, the chromatographic behavior of the titania which had rutile as a major phase should be further studied. It will give more information of separation mechanism of titania stationary phase in TLC. Moreover, the comparison of separation efficiency of electrospun fibrous titania TLC to a similar format of stationary phase such as monolith structure or electrospun fibrous silica should be examined.

The shrinkage of the fiber after calcination caused the detachment of the electrospun fibrous titania from the TLC plate. The method of titania preparation should be modified in order to reduce the shrinkage of the fibers.

## References

- [1] Hauck, H., Bund, O., Fischer, W., and Schulz, M. Ultra-thin layer chromatography (UTLC) — A new dimension in thin-layer chromatography. JPC - Journal of Planar Chromatography - Modern TLC 14 (2001): 234-236.
- [2] Powell, S.C. Ultrathin-layer chromatography spotting and detection on the sub-millimeter scale. Analytical Chemistry 82 (2010): 3408-3408.
- [3] Vovk, I., Popović, G., Simonovska, B., Albrecht, A., and Agbaba, D. Ultra-thin-layer chromatography mass spectrometry and thin-layer chromatography mass spectrometry of single peptides of angiotensin-converting enzyme inhibitors. Journal of Chromatography A 1218 (2011): 3089-3094.
- [4] Bezuidenhout, L.W. and Brett, M.J. Ultrathin layer chromatography on nanostructured thin films. Journal of Chromatography A 1183 (2008): 179-185.
- [5] Clark, J.E. and Olesik, S.V. Technique for Ultrathin Layer Chromatography Using an Electrospun, Nanofibrous Stationary Phase. Analytical Chemistry 81 (2009): 4121-4129.
- [6] Clark, J.E. and Olesik, S.V. Electrospun glassy carbon ultra-thin layer chromatography devices. Journal of Chromatography A 1217 (2010): 4655-4662.
- [7] Nawrocki, J., Dunlap, C., McCormick, A., and Carr, P.W. Part I. Chromatography using ultra-stable metal oxide-based stationary phases for HPLC. Journal of Chromatography A 1028 (2004): 1-30.
- [8] Winkler, J. and Marmé, S. Titania as a sorbent in normal-phase liquid chromatography. Journal of Chromatography A 888 (2000): 51-62.
- [9] Chandrasekar, R., Zhang, L., Howe, J., Hedin, N., Zhang, Y., and Fong, H. Fabrication and characterization of electrospun titania nanofibers. Journal of Materials Science 44 (2009): 1198-1205.
- [10] Chen, J.-Y., Chen, H.-C., Lin, J.-N., and Kuo, C. Effects of polymer media on electrospun mesoporous titania nanofibers. Materials Chemistry and Physics 107 (2008): 480-487.

- [11] Chuangchote, S., Jitputti, J., Sagawa, T., and Yoshikawa, S. Photocatalytic Activity for Hydrogen Evolution of Electrospun TiO<sub>2</sub> Nanofibers. ACS Applied Materials & Interfaces 1 (2009): 1140-1143.
- [12] Jabal, J.M.F., McGarry, L., Sobczyk, A., and Aston, D.E. Wettability of Electrospun Poly(vinylpyrrolidone)-Titania Fiber Mats on Glass and ITO Substrates in Aqueous Media. ACS Applied Materials & Interfaces 1 (2009): 2325-2331.
- [13] Jeerapong, W., Varong, P., and Pitt, S. Titanium (IV) oxide nanofibers by combined sol-gel and electrospinning techniques: preliminary report on effects of preparation conditions and secondary metal dopant. Science and Technology of Advanced Materials 6 (2005): 240.
- [14] Li, D. and Xia, Y. Fabrication of Titania Nanofibers by Electrospinning. Nano Letters 3 (2003): 555-560.
- [15] Meng, X., Luo, N., Cao, S., Zhang, S., Yang, M., and Hu, X. In-situ growth of titania nanoparticles in electrospun polymer nanofibers at low temperature. Materials Letters 63 (2009): 1401-1403.
- [16] Park, S.-J., Chase, G., Jeong, K.-U., and Kim, H. Mechanical properties of titania nanofiber mats fabricated by electrospinning of sol-gel precursor. Journal of Sol-Gel Science and Technology 54 (2010): 188-194.
- [17] Andrady, A.L. Science and Technology of Polymer Nanofibers. New Jersey: John Wiley & Sons, Inc., 2008.
- [18] Ramakrishna, S., Fujihara, K., Teo, W.E., Lim, T.C., and Ma, Z. An Introduction to Electrospinning and Nanofibers. Singapore: World Scientific Publishing Co. Pte. Ltd., 2005.
- [19] Deitzel, J.M., Kleinmeyer, J., Harris, D., and Beck Tan, N.C. The effect of processing variables on the morphology of electrospun nanofibers and textiles. Polymer 42 (2001): 261-272.
- [20] Chuangchote, S., Sagawa, T., and Yoshikawa, S. Electrospinning of poly(vinyl pyrrolidone): Effects of solvents on electrospinnability for the fabrication of poly(*p*-phenylene vinylene) and TiO<sub>2</sub> nanofibers. Journal of Applied Polymer Science 114 (2009): 2777-2791.

- [21] Lee, J.-S., Lee, Y.-I., Song, H., Jang, D.-H., and Choa, Y.-H. Synthesis and characterization of TiO<sub>2</sub> nanowires with controlled porosity and microstructure using electrospinning method. Current Applied Physics 11 (2011): S210-S214.
- [22] Chowdhury, M. and Stylios, G. Effect of experimental parameters on the morphology of electrospun Nylon 6 fibres. IJBAS: International Journal of Basic & Applied Sciences 10 (2012): 116-131.
- [23] Joon, P.J., Youn, M.L., and Young, C.N. Study on morphology of electrospun poly(carpolactone) nanofiber. Journal of Industrial and Engineering Chemistry 11 (2005): 573-578.
- [24] Biber, E., Gündüz, G., Mavis, B., and Colak, U. Effects of electrospinning process parameters on nanofibers obtained from Nylon 6 and poly (ethylene-*n*-butyl acrylate-maleic anhydride) elastomer blends using Johnson S<sub>B</sub> statistical distribution function. Applied Physics A: Materials Science & Processing 99 (2010): 477-487.
- [25] Supapol, J. Detailed investigation on titanium (IV) oxide nanofiber synthesized by combined sol-gel and electrospinning techniques. Master's Thesis. Department of Chemical Engineering, Chulalongkorn University, 2007.
- [26] Khataee, A. and Mansoori, G.A. Nanostructured Titanium Dioxide Materials: Properties, Preparation and Applications. Singapore: World Scientific Publishing Co. Pte. Ltd., 2011.
- [27] Kataoka, S., Gurau, M.C., Albertorio, F., Holden, M.A., Lim, S.-M., Yang, R.D., and Cremer, P.S. Investigation of Water Structure at the TiO<sub>2</sub>/Aqueous Interface. Langmuir 20 (2004): 1662-1666.
- [28] Parfitt, G.D. Surface chemistry of oxides. Pure and Applied Chemistry 48 (1976): 415-418.
- [29] Kosmulski, M. A literature survey of the differences between the reported isoelectric points and their discussion. Colloids and Surfaces A: Physicochemical and Engineering Aspects 222 (2003): 113-118.
- [30] Kao, L.-H., Hsu, T.-C., and Lu, H.-Y. Sol-gel synthesis and morphological control of nanocrystalline TiO<sub>2</sub> via urea treatment. Journal of Colloid and Interface Science 316 (2007): 160-167.



- [31] Jorge, M.-V., Manuel, S.-C., Claudio, F.-R., and Sergio, C. Formation of smooth and rough TiO<sub>2</sub> thin films on fiberglass by sol-gel method. Journal of the Mexican Chemical Society 50 (2006): 8-13.
- [32] Mehrizad, A., Gharbani, P., and Tabatabaii, S.M. Synthesis of nanosized TiO<sub>2</sub> powder by Sol-Gel method in acidic conditions. Journal of the Iranian Chemical Resaerch 2 (2009): 145-149.
- [33] Kim, K.D. and Kim, H.T. Synthesis of TiO<sub>2</sub> nanoparticles by hydrolysis of TEOT and decrease of particle size using a two-stage mixed method. Powder Technology 119 (2001): 164-172.
- [34] Neppolian, B., Wang, Q., Jung, H., and Choi, H. Ultrasonic-assisted sol-gel method of preparation of TiO<sub>2</sub> nano-particles: Characterization, properties and 4-chlorophenol removal application. Ultrasonics Sonochemistry 15 (2008): 649-658.
- [35] Su, C., Hong, B.Y., and Tseng, C.M. Sol-gel preparation and photocatalysis of titanium dioxide. Catalysis Today 96 (2004): 119-126.
- [36] Sayilkan, F., Asiltürk, M., Sayilkan, H., Önal, Y., Akarsu, M., and Arpaç, E. Characterization of TiO<sub>2</sub> Synthesized in Alcohol by a Sol-Gel Process: The Effects of Annealing Temperature and Acid Catalyst. Turkish Journal of Chemistry 29 (2005): 697-706.
- [37] Li, Y., White, T.J., and Lim, S.H. Low-temperature synthesis and microstructural control of titania nano-particles. Journal of Solid State Chemistry 177 (2004): 1372-1381.
- [38] Touchstone, J.C. Practice of Thin-Layer Chromatography New York: Wiley-Interscience, 1992.
- [39] Elke, H.-D. Applied Thin Layer Chromatography. Best Practice and Avoidance of Mistakes. Weinheim: Wiley-VCH, 2000.
- [40] Sherma, J. and Fried, B. Handbook of Thin-Layer Chromatography. 3<sup>rd</sup> ed. New York: Marcel Dekker, Inc., 2003.
- [41] Žižkovský, V., Kučera, R., Klimeš, J., and Dohnal, J. Titania-based stationary phase in separation of ondansetron and its related compounds. Journal of Chromatography A 1189 (2008): 83-91.

- [42] Abi Jaoudé, M. and Randon, J. Capillary monolithic titania column for miniaturized liquid chromatography and extraction of organo-phosphorous compounds. Analytical and Bioanalytical Chemistry 400 (2011): 1241-1249.
- [43] Grün, M., Kurganov, A.A., Schacht, S., Schüth, F., and Unger, K.K. Comparison of an ordered mesoporous aluminosilicate, silica, alumina, titania and zirconia in normal-phase high-performance liquid chromatography. Journal of Chromatography A 740 (1996): 1-9.
- [44] Hauck, H. and Schulz, M. Ultra thin-layer chromatography. Chromatographia 57 (2003): S313-S315.
- [45] Bakry, R., Bonn, G.K., Mair, D., and Svec, F. Monolithic Porous Polymer Layer for the Separation of Peptides and Proteins Using Thin-Layer Chromatography Coupled with MALDI-TOF-MS. Analytical Chemistry 79 (2006): 486-493.
- [46] Sing, K.S.W., Everett, D.H., Haul, R.A.W., Moscou, L., Pierotti, R.A., Rouquerol, J., and Siemieniewska, T. Reporting physisorption data for gas/solid systems with special reference to the determination of surface area and porosity (Recommendations 1984). Pure and Applied Chemistry 57 (1985): 603-619.
- [47] Zdravkov, B., Čermák, J., Šefara, M., and Janků, J. Pore classification in the characterization of porous materials: A perspective. Central European Journal of Chemistry 5 (2007): 385-395.
- [48] Yu, J., Yu, J.C., Leung, M.K.P., Ho, W., Cheng, B., Zhao, X., and Zhao, J. Effects of acidic and basic hydrolysis catalysts on the photocatalytic activity and microstructures of bimodal mesoporous titania. Journal of Catalysis 217 (2003): 69-78.
- [49] Jung, K.Y. and Park, S.B. Anatase-phase titania: preparation by embedding silica and photocatalytic activity for the decomposition of trichloroethylene. Journal of Photochemistry and Photobiology A: Chemistry 127 (1999): 117-122.
- [50] Zhao, J., Wang, Z., Wang, L., Yang, H., and Zhao, M. The preparation and mechanism studies of porous titania. Materials Chemistry and Physics 63 (2000): 9-12.

## VITA

Miss Supamas Kanjanakunthon was born on July 18, 1986 in Samut Sakhon, Thailand. She graduated with a Bachelor of Science degree in Chulalongkorn University in 2009. After that, she has been a graduate student at the Program of Petrochemistry and Polymer Science, Chulalongkorn University, and become a member of Chromatography and Separation Research Unit. She finished her Master's degree of Science in May 2012.

### **Poster presentation and proceeding**

“ELECTROSPUN TITANIUM DIOXIDE FIBROUS STATIONARY PHASE FOR THIN LAYER CHROMATOGRAPHY” Supamas Kanjanakunthon, Nipaka Sukpirom and Puttaruksa Varanusupakul. Poster presentation and proceeding, *Pure and Applied Chemistry International Conference 2012 (PACCON 2012)*, The Empress Hotel, Chiang Mai, Thailand, 11-13 January, 2012.